

Ultra-High-Efficiency Aluminum Production Cell

About Argonne National Laboratory

Argonne is a U.S. Department of Energy laboratory managed by UChicago Argonne, LLC under contract DE-AC02-06CH11357. The Laboratory's main facility is outside Chicago, at 9700 South Cass Avenue, Argonne, Illinois 60439. For information about Argonne and its pioneering science and technology programs, see www.anl.gov.

DOCUMENT AVAILABILITY

Online Access: U.S. Department of Energy (DOE) reports produced after 1991 and a growing number of pre-1991 documents are available free via DOE's SciTech Connect (<http://www.osti.gov/scitech/>)

Reports not in digital format may be purchased by the public from the National Technical Information Service (NTIS):

U.S. Department of Commerce
National Technical Information Service
5301 Shawnee Rd
Alexandria, VA 22312

www.ntis.gov

Phone: (800) 553-NTIS (6847) or (703) 605-6000

Fax: (703) 605-6900

Email: orders@ntis.gov

Reports not in digital format are available to DOE and DOE contractors from the Office of Scientific and Technical Information (OSTI):

U.S. Department of Energy
Office of Scientific and Technical Information
P.O. Box 62
Oak Ridge, TN 37831-0062

www.osti.gov

Phone: (865) 576-8401

Fax: (865) 576-5728

Email: reports@osti.gov

Disclaimer

This report was prepared as an account of work sponsored by an agency of the United States Government. Neither the United States Government nor any agency thereof, nor UChicago Argonne, LLC, nor any of their employees or officers, makes any warranty, express or implied, or assumes any legal liability or responsibility for the accuracy, completeness, or usefulness of any information, apparatus, product, or process disclosed, or represents that its use would not infringe privately owned rights. Reference herein to any specific commercial product, process, or service by trade name, trademark, manufacturer, or otherwise, does not necessarily constitute or imply its endorsement, recommendation, or favoring by the United States Government or any agency thereof. The views and opinions of document authors expressed herein do not necessarily state or reflect those of the United States Government or any agency thereof.

Ultra-High-Efficiency Aluminum Production Cell

by

John N. Hryn, Olga Y. Tkacheva and Jeffrey S. Spangenberg
Energy Systems Division, Argonne National Laboratory

Project team member organizations:

Kingston Process Metallurgy

Noranda Aluminum

DOE Award Number DE-AC02-06CH11357, CPS Agreement 18992

Project Period: 10/2009 – 10/2012

April 2014

This page intentionally left blank

CONTENTS

EXECUTIVE SUMMARY	1
1 INTRODUCTION	5
2 BACKGROUND	7
2.1 Electrolyte Chemistry	7
2.2 Anode and Cathode Materials	7
2.3 Cell Design	8
2.4 Low-Temperature Aluminum Electrolysis in Potassium-Cryolite-Based Electrolytes	8
2.5 Goals and Objectives.....	10
3 RESULTS AND DISCUSSION.....	11
3.1 Experimental Work	11
3.1.1 Setup for 20-A and 100-A cells	11
3.1.2 Electrolyte	14
3.2 20-A Electrolysis Testing	22
3.2.1 Operating Parameters.....	22
3.2.2 Current Efficiency.....	24
3.2.3 Voltage Anomalies	25
3.2.4 State of the Anode Surface before Electrolysis	31
3.2.5 Purity of the Produced Aluminum Metal.....	34
3.3 100-A Electrolysis Testing	38
3.3.1 Oxygen Content in Outlet Gas	38
3.3.2 Operating Parameters of the 100-A Electrolysis	39
3.3.3 Thickness of the Anode Scale	43
3.4 Material Testing	44
3.4.1 Material Sample Testing	44
3.4.2 Material Testing at Electrolysis Conditions	46
3.5 1,000-A Electrolysis Test	47
4 BENEFITS ASSESSMENT	53
5 COMMERCIALIZATION	57
6 ACCOMPLISHMENTS	59
7 CONCLUSIONS	61
8 RECOMMENDATIONS.....	63

CONTENTS (Cont.)

9 REFERENCES 65
APPENDIX A: Operating Parameters..... 69

ACRONYMS

ACD	anode-to-cathode distance
CE	current efficiency
CE _{Al}	current efficiency determined based on produced aluminum mass
CE _{Ox}	current efficiency determined based on oxygen concentration in outlet gas
CR	cryolite ratio
DOE	U.S. Department of Energy
GC	gas chromatography
GHG	greenhouse gas
E _A	potential between reference electrode and anode
E _C	potential between reference electrode and cathode
EDS	energy dispersive spectroscopy
i _a	anode current density
i _c	cathode current density
ICP	inductively coupled plasma
MS	mass spectrometry
OES	optical emission spectrometry
SEM	scanning electron microscopy
SS	stainless steel
XRD	x-ray diffraction

FIGURES

1	Schematic of experimental cell.....	12
2	20-A experimental setup with two wetted cathodes and one aluminum bronze anode	12
3	Top view of assembled water-cooled furnace-tube end-cap.....	12
4	Experimental facility	12
5	Sketch of the outlet gas scrubber system.....	13
6	Oxygen in outgas flow during first hours of electrolysis for KF-AlF ₃ at 700°C and for KF-AlF ₃ + NaF at 730°C.....	16
7	Content of silicon in KF-AlF ₃ electrolyte in 100-A electrolysis at 750°C	17
8	Measured and calculated sodium concentrations during 20-A electrolysis in KF-AlF ₃ at 700°C and in KF-AlF ₃ + NaF at 700°C and at 750°C.....	17
9	Measured CR and concentration of alumina and sodium in electrolyte during 100-A electrolysis in KF-AlF ₃ at 750°C	18
10	Measured and calculated concentrations of AlF ₃ and KF during electrolysis in electrolyte KF-AlF ₃ , CR of 1.37, at 700°C	19
11	Measured and calculated CR in electrolyte KF-AlF ₃ , CR of 1.37, at 700°C	19
12	Alumina content in the electrolytes during 20-A electrolysis	20
13	Optical image of the surface showing the translucent crystals covering the anode surface; SEM image of surface crystals; and graph of corresponding EDS spectrum	20
14	Liquidus temperatures of electrolyte, measured and available data [36]	21
15	Operating parameters of 20-A electrolysis in KF-AlF ₃ electrolyte	22
16	Enhanced plot of temperature change and voltage oscillation in 20-A electrolysis	22
17	Electrolysis plot in a 20-A cell with vertical graphite anode and two graphite cathodes, in KF-AlF ₃ electrolyte with a CR of 1.3.....	23
18	Aluminum bronze anode after 20-A electrolysis in KF-AlF ₃	23
19	Current efficiency and operating parameters of electrolysis in KF-AlF ₃ at 750°C	25
20	Effect of cathode and anode processes on voltage during electrolysis in KF-AlF ₃ -NaF electrolyte	26
21	Plot of electrolysis in KF-AlF ₃ -NaF at 4 wt%, with a CR of 1.3 at 700°C.....	26
22	Electrodes after electrolysis in KF-AlF ₃ -NaF at 4 wt% at 700°C.....	27
23	Cathode deposit: gray external layer and black internal layer.....	27
24	XRD spectrum of the cathode deposit.....	27
25	Plot of electrolysis in KF-AlF ₃ -NaF at 4 wt%, with a CR of 1.3 at 700 and 750°C.....	27
26	Electrodes after electrolysis in KF-AlF ₃ -NaF at 4 wt%) at 750°C.....	27

27	Enhanced plot of electrolysis in KF–AlF ₃ -NaF	28
28	Parameters of electrolysis in KF-AlF ₃ electrolyte during the first 5 hours	29
29	Decrease of voltage and anode potential values due to anode corrosion.....	29
30	Corroded anode after electrolysis in KF-AlF ₃ electrolyte at 730°C.....	29
31	Voltage rise due to anode passivation during electrolysis in KF-AlF ₃ -NaF electrolyte.....	30
32	Anode covered with spongy-like scale after electrolysis in KF-AlF ₃ -NaF electrolyte at 750°C.....	30
33	Voltage drops, which indicate the contact of the anode with aluminum metal.....	30
34	Half of the anode dissolved in aluminum metal.....	30
35	Aluminum produced in Experiment EAL10.....	30
36	Plot of electrolysis in KF-AlF ₃ electrolyte at 750°C	31
37	Anode after electrolysis in Experiment E36.....	31
38	Aluminum bronze samples covered with black scale after exposure above the electrolyte. Detached scale from Sample N2	33
39	XRD spectra of the scale	34
40	Content of copper, iron, and silicon in overall aluminum during electrolysis at 700°C and 750°C	35
41	Aluminum bronze anodes after 48 hours of electrolysis in KF-AlF ₃ : A at 700°C, B at 750°C.....	36
42	Copper content in the instantaneous aluminum metal produced during 20-A tests of Groups II and III	37
43	Copper content in the instantaneous aluminum metal produced in KF-AlF ₃ electrolyte at 750°C at different current densities.....	38
44	Oxygen sensor reading during 100-A electrolysis	39
45	Operating parameters of 100-A electrolysis in KF-AlF ₃ electrolyte.....	40
46	Electrodes, aluminum metal, and electrolyte cooled in the alumina crucible after 110 hours of 100-A electrolysis, showing cathode in contact with aluminum	40
47	Anode scale separated from the anode during cooling	40
48	Aluminum bronze anode after 25 hours of 100-A electrolysis, showing that the anode scale spalled out during cooling	40
49	Asymmetrical change of voltage and temperature during a 100-A test	41
50	Aluminum bronze anode after 100-A test, showing aluminum metal droplets on the anode surface	41
51	Operating parameters of 100-A electrolysis in KF-AlF ₃ electrolyte.....	42
52	Asymmetrical change in voltage and temperature	42

53	Thickness of the anode scale formed during 20-A, 100-A, and 1,000-A tests.....	43
54	XRD spectra of anode scale obtained on the internal side and external side sides.....	44
55	Views of BN sample exposed to KF-AlF ₃ electrolyte and molten aluminum at 750°C after 0, 178, 410, 575, and 950 hours	45
56	Thickness of the BN sample exposed to the KF-AlF ₃ electrolyte and molten aluminum at 750°C for 950 hours.....	46
57	View from above of a BN crucible with molten electrolyte inside a stainless steel shell placed in a furnace.....	47
58	BN crucible inside of the stainless steel shell placed in the furnace	48
59	Bus bars for anodes and cathodes.....	48
60	Scrubber purification system	48
61	View of furnace when electrolysis is in progress.....	48
62	Shroud mounted on furnace supporting system of electrodes and bus bars	48
63	Plot of the 1,000-A electrolysis	49
64	Changes in voltage, alumina content in the electrolyte, CR, and energy expended on maintaining the furnace's heat during 1,000-A electrolysis.....	49
65	After electrolysis, electrodes suspended above melt	50
66	Cooling electrodes about to be mounted on shroud	50
67	Resistivity of the electrolyte and molten aluminum vs. distance from the bottom of the crucible	51

TABLES

1	Content of impurities, excluding alumina, in aluminum fluoride.....	15
2	Content of impurities in alumina	15
3	Liquidus temperatures of electrolytes measured in the electrolysis cell.....	21
4	Current efficiency based on the evolved oxygen and produced aluminum contents in 20-A tests	24
5	Parameters for 20-A electrolysis testing	32
6	Copper content in the overall and instantaneous aluminum.....	35
7	Conditions and results of material tests in the KF-AlF ₃ Al ₂ O ₃ -saturated electrolyte with a CR of 1.3 at 750°C.....	45
8	U.S. energy requirements for aluminum production	53
A-1	Operating parameters for the completed 20-A electrolysis tests.....	69
A-2	Operating parameters for the completed 100-A electrolysis tests.....	72

This page intentionally left blank

ULTRA-HIGH-EFFICIENCY ALUMINUM PRODUCTION CELL

by

John N. Hryn

EXECUTIVE SUMMARY

The industrial production of aluminum is based on the Hall-Heroult electrolysis process. In this process, alumina is dissolved in an electrolytic cell containing a molten sodium-cryolite-based electrolyte at 970°C. The alumina is electrolytically reduced to aluminum metal at the cathode when electric current is applied to the electrolytic cell. At the anode, electrolytic oxygen reacts with the carbon anodes, producing carbon dioxide (CO₂), which is emitted from the cell. The process suffers from many inefficiencies, primarily because the carbon anodes are continuously consumed during electrolysis, which increases the anode-to-cathode distance and subsequent increased voltage drop across the cell. The search for nonconsumable, or inert anodes, has been a challenge to the industry because the high temperature and corrosive environment of the electrolytic cell severely limits choices for candidate inert anode materials. Another inefficiency of the process results from the use of a carbon cathode that is not wetted by aluminum metal. This causes a deep aluminum molten metal pool to form on the cathode, which fluctuates in the presence of strong magnetic fields in the cell. To ensure that the anode and cathode do not touch, the anode-to-cathode distance (ACD) is increased, again resulting in an increased voltage drop across the cell. The constant corrosion of the cell materials and high energy requirements that are associated with the high temperatures used for electrolysis, the inefficient cell design, and the production of CO₂ (which contributes to greenhouse gas emissions) are some of the current problems that reveal the need to improve conventional electrolysis processes.

In this study, a systems approach was used to develop an ultra-high-efficiency aluminum production cell. The approach was to change the:

- Electrolyte chemistry, thus allowing for a lower operating temperature;
- Anode and cathode materials, since more material options are available with a lower operating temperature; and
- Configuration to a vertical bipolar cell, since inert anodes enable new energy-efficient cell designs.

The traditional electrolyte chemistry was modified to allow for a lower operating temperature in order to enhance efficiency and reduce metal anode corrosion. Normally, lower-temperature processes are achieved by using additives and decreasing the cryolite ratio (CR). However, such modifications come at the expense of decreases in the solubility of alumina, the alumina dissolution rate, and the electrical conductivity. The only exception is the addition of potassium fluoride (KF), which, when used under the same process conditions, yields increases in the solubility of alumina and the alumina dissolution rate. Low electrical conductivity can be improved by altering the configuration electrolysis cell; vertical rather than horizontal electrode placement yields higher electrical conductivity and energy efficiency. However, when a potassium-based electrolyte is used, sodium (which is present as sodium fluoride [NaF] in the electrolyte) is introduced to the electrolytic cell as an impurity in the alumina feed, and this

sodium can build up over time. It has been determined that the presence of NaF above 2 weight percent (wt%) in the electrolyte has a detrimental effect on the anode structure and the electrolytic process.

Another modification that was made was a change in the anode and cathode materials, since the material options were less restricted because of the lower electrolysis temperature. To eliminate anode consumption and CO₂ emissions, degradable carbon anodes were replaced with inert anodes. Several alloys were evaluated. Aluminum bronze consistently performed better than did other materials. A wetted dripping cathode (various metals) was used, since the most important requirement for cathodes is good wettability between the cathode surface and the formed molten aluminum.

Hence, the general scope of this project was to run small-scale tests using a 20-A cell to determine the optimal electrolysis conditions and design that would enhance energy efficiency, to resolve issues such as NaF buildup in the cells, and to demonstrate sustained cell operation in long-term tests in a 100-A cell. All results were used to design and conduct experiments in a larger, semi-industrial-scale, 1,000-A cell.

For the initial tests, a 20-A cell was vertically fitted with an aluminum bronze anode and two wetted cathodes in KF-AlF₃ (aluminum fluoride) or KF-AlF₃-NaF (2–4 wt%) electrolytes with a CR of 1.3 at a temperature range of 700–770°C. Typically, the anode current density was 0.45 A/cm², and the cathode current density was 0.52 A/cm². The distance between the anode and cathode was 2 cm. Overall, the operational voltage and cathode and anode potentials of the electrolysis system were stable. The oxygen level in the outlet gas was also stable; this was used as an indicator to confirm the smooth course of electrolysis. The alumina content in the electrolyte was 4.5 wt%, on average. To eliminate the NaF issue, the operating temperature was adjusted. It was determined that the minimal operating temperatures for electrolysis in KF-AlF₃-NaF electrolytes at 2 wt% and 4 wt% should be as high as 750°C and 770°C, respectively.

The quality of produced aluminum in the 20-A cell was analyzed, and metal impurities (e.g., potassium, chromium, manganese, nickel) were not found in it. (The concentration was found to be less than the detectable limit of inductively coupled plasma-optical emission spectrometry [0.05 wt%] at any time during electrolysis.) However, copper, iron, and silicon were found. It was determined that the higher the process's current efficiency was, the better the quality of the produced aluminum was. Furthermore, if the anode surface was not in contact with the electrolyte vapors before it was immersed in the electrolyte, the aluminum produced in the early stages of electrolysis did not contain any impurities.

The 100-A cell was used to perform long-term electrolysis tests and determine the impacts of the tests on the cell materials. All experiments were performed by using the KF-AlF₃ electrolyte with a CR of 1.3 in a cell with one aluminum bronze anode and two wetted cathodes at a temperature that varied between 730 and 750°C. The anode current density was 0.45 A/cm², the cathode current density was 0.52 A/cm², and the anode-to-cathode distance was 2 cm. Long-term tests were performed for more than 100 hours with an alumina concentration of about 5.5 wt%. Information gathered from 20-A tests indicated that the 100-A cell electrolysis process resulted in mostly stable conditions, producing aluminum that was not contaminated. It was determined that the anode process controlled the voltage. The aluminum bronze anode performed very well in low-temperature electrolysis with potassium cryolite.

Before the 1,000-A semi-industrial electrolysis cell was developed, several ceramics to be used as construction materials were tested for their compatibility with the electrolyte and harsh electrolysis conditions (KF-AlF₃, CR of 1.3, 750°C). Boron nitride (grade AX05) was able to withstand electrolysis heating and cooling without any signs of corrosion and was most protective to stainless steel cell components.

Aluminum electrolysis was performed at a current of 1,000 A, at a temperature of 750°C, and in a cell fitted with vertically orientated aluminum bronze anodes and wetted cathodes. The cell included a total of six anodes and cathodes with a current density of 0.5 A/cm² and an ACD of 2.2 cm. The 1,000-A test was successfully performed to demonstrate cell operation at a semi-industrial scale. The electrolysis was sustained, and no voltage fluctuation was observed.

This page intentionally left blank

1 INTRODUCTION

Presently, aluminum metal is produced by the 120-year-old Hall-Heroult electrolysis process. In this process, electrolysis is performed at a high temperature of 970°C by using molten sodium-cryolite-based electrolyte (sodium fluoride-aluminum fluoride [NaF-AlF₃]), which serves as a solvent for alumina (Al₂O₃). An electrical current is passed through the cell between the carbon anode and cathode. The high-temperature operation results in excessive corrosion of the cell materials. During electrolysis, the carbon anode is consumed, forming carbon dioxide (CO₂) gas, which contributes to the greenhouse gas (GHG) emissions and energy inefficiency due to the changing anode shape. Use of the carbon cathode, nonwetted, requires an excessive anode-to-cathode distance (ACD) and contributes to energy inefficiency due to the large cell voltage drop. The horizontal Hall-Heroult cell configuration (as opposed to the vertical bipolar configuration) entails a larger cell footprint, which contributes to energy inefficiency due to excessive heat loss.

To improve the energy efficiency of the conventional Hall-Heroult aluminum technology, the main challenge is to replace consumable carbon anodes with nonconsumable inert anodes. Thus far, there has been no information concerning the successful implementation of inert anodes in conventional aluminum electrolysis [1]. The high operating temperatures used in current practice are a significant factor affecting anode and material stability.

A new approach to energy-efficient aluminum production was conceived and investigated during a 3-year project (2001–2004) sponsored by the U.S. Department of Energy (DOE), Office of Energy Efficiency and Renewable Energy (EERE), Industrial Technologies Program (ITP). The work was done by a team composed of researchers from Argonne National Laboratory, KPM, and Noranda Aluminum. The approach that was developed involved the following pathways:

- Changing the electrolyte chemistry, thus allowing for a lower operating temperature;
- Changing the anode and cathode materials, since more material options are available with a lower operating temperature; and
- Changing the configuration to a vertical bipolar cell, since inert anodes enable new energy-efficient cell designs.

This page intentionally left blank

2 BACKGROUND

2.1 ELECTROLYTE CHEMISTRY

According to the literature, initial attempts to develop a low-temperature process focused on modifying the conventional sodium-cryolite (Na_3AlF_6)-based electrolyte through the addition of potassium fluoride (KF), lithium fluoride (LiF), and aluminum fluoride (AlF_3), along with some other additives. Furthermore, decreasing the cryolite ratio (CR) was a basic area of focus. In fact, all potential additives to sodium cryolite can reduce the liquidus temperature [2]. However, any addition, except KF, decreases alumina solubility [3, 4]. Therefore, the main disadvantages of electrolytes based on sodium cryolite with a low CR are low alumina solubility, a low alumina dissolution rate, and low electrical conductivity [5].

Argonne National Laboratory proposed to use potassium cryolite as an electrolyte for aluminum electrolysis. A KF- AlF_3 molten system with a CR of 1.3 and concentration of 5 weight percent (5 wt%) dissolved alumina allows electrolysis to be carried out at a temperature as low as 700°C [6]. The main advantages of potassium cryolite (K_3AlF_6) over sodium cryolite at temperatures below 800°C are the relatively high solubility of alumina [7–9] and its high rate of dissolution [8]. For KF- AlF_3 melts with a CR of 1.3 to 1.5, the values of alumina solubility in the 700 – 800°C temperature range are comparable with the operational alumina concentration in a conventional sodium-cryolite-based bath. However, new issues arise. Sodium, present as sodium fluoride (NaF) in the electrolyte, is introduced to the electrolytic cell as an impurity in the alumina feed and can build up over time. It was determined that the presence of NaF above 2 wt% in the electrolyte is likely to have a detrimental effect on anode wear and on the operating parameters [10].

The main disadvantage of the potassium-cryolite-based electrolyte over the conventional sodium system is its lower electrical conductivity [5, 11]. It cannot be compensated for by simply modifying the electrolyte with additives that are more conductive. However, it can be improved by altering the electrolysis cell.

2.2 ANODE AND CATHODE MATERIALS

Of all the known types of inert anodes, such as metals, ceramics, and cermets, the metal alloy anodes have the most-promising features for industrial implementation. For successful use in aluminum production, inert anodes must satisfy certain requirements, such as low solubility in cryolite melts, high electrical conductivity, high physical stability, and affordable cost. Metal anodes are well-suited to satisfy these requirements since they are good electrical conductors and can be machined to a desired shape from readily available materials.

At Argonne, several commercially available alloys were evaluated as inert anodes in electrolysis tests using KF- AlF_3 melts at 700°C [6]. It was found that aluminum bronze (in standard bronze, tin rather than aluminum is the chief alloy added to copper) consistently performed better than the other alloys.

Cathodes must be thermally and chemically stable under electrolysis conditions, but the most important requirement is good wettability between the cathode surface and formed molten aluminum. To date, titanium diboride (TiB_2) or TiB_2 -C composites are considered to be the most favorable cathode materials.

2.3 CELL DESIGN

Inert anodes and wetted dripping cathodes allow changes in the bath construction and the use of vertical electrodes. An electrolysis cell fitted with vertical electrodes enables the use of several electrodes in a relatively small bath volume. One advantage of this design is that the vertical orientation electrode provides a reduction in the anode current density. Another is the ability to reduce the operating voltage by decreasing the ACD, which will allow for increased amperage and efficiency while maintaining a low anode current density. Furthermore, the use of vertical electrodes eliminates the need to adjust the anode position in the bath during electrolysis, which minimizes cell intervention. Such cells are described in several U.S. patents [12–14].

2.4 LOW-TEMPERATURE ALUMINUM ELECTROLYSIS IN POTASSIUM-CRYOLITE-BASED ELECTROLYTES

Initially, Argonne National Laboratory successfully demonstrated aluminum electrolysis in a cell with a vertically oriented aluminum bronze anode and TiB_2 -based cathode using a KF-AlF_3 electrolyte with a CR of 1.3 at 700°C [6]. Electrolysis was performed in 10-, 20-, and 100-A cells with anode current densities of about 0.45 A/cm^2 . Current efficiencies of about 85% were reached, and the purity of the aluminum product was better than 99.5% at times.

Argonne's promising demonstration of low-temperature electrolysis with potassium cryolite electrolyte in a cell fitted with inert anodes encouraged other laboratories to research and develop this emerging technology [15–28].

Researchers in *Central South University, Changsha, China*, studied the corrosive behavior of inert cermet anodes in potassium-cryolite-based electrolytes and the sodium issue [15–20].

Electrolysis in a KF-AlF_3 (CR of 1.3) and $\text{K}_3\text{AlF}_6\text{-Na}_3\text{AlF}_6\text{-AlF}_3$ bath at 700°C was accompanied by a high and unsteady voltage. It was pointed out [16] that the low-temperature electrolysis was more sustained in the KF-NaF-AlF_3 ($\text{KF:NaF} = 1:1$) electrolyte with a CR of 1.5 at 800°C as opposed to the high, unstable, fluctuating voltage (5.96–19.6 V) observed at 700°C . The voltage fluctuation was explained by the formation of cathode encrustation. The $\text{Cu}/(\text{NiO-NiFe}_2\text{O}_4)$ cermet anode's behavior in $\text{K}_3\text{AlF}_6\text{-Na}_3\text{AlF}_6$ -based electrolytes was continued to be studied at a temperature range of $740\text{--}960^\circ\text{C}$ [19]. Electrolysis was performed at a current density of 1 A/cm^2 over 6 hours, with an ACD of 30 mm. The tested anodes exhibited the best properties at an electrolysis temperature of $830\text{--}840^\circ\text{C}$. It was reported that the total percentage of impurities in the produced aluminum amounted to $<0.3 \text{ wt}\%$.

Work at the *Institute of High Temperature Electrochemistry (IHTE), Yekaterinburg, Russia*, focused on the fundamental properties of potassium-cryolite-based electrolytes and on testing cermet and metal inert anodes under low-temperature electrolysis conditions [21–28].

The aluminum electrolysis at 700°C in cells with KF-AlF_3 electrolytes (CR of 1.3) and cermet or metal anodes was complicated by salt passivation on the electrodes due to a change in the electrolyte composition. Increasing the CR to 1.5 and the temperature to 800°C and modifying the bath composition allowed for stable aluminum electrolysis in an NaF-KF-LiF-AlF_3 electrolyte (12-30-3-55 wt%). A test using $\text{Cu}_x\text{-Ni}_y\text{-Fe}_z$ anodes was carried out in an electrolyte containing a high concentration of NaF, with a composition of $\text{NaF-KF-AlF}_3\text{-CaF}_2\text{-Al}_2\text{O}_3$ (34-12-50-4-saturated wt%), a CR of 1.8, and at a temperature of 850°C . However, in an electrolysis test conducted in

electrolytes based on potassium cryolite at 790°C, the anodes being tested performed better [22, 28]. The current density was 0.5 A/cm², and the test durations varied from 72 to 96 hours. The voltage during electrolysis changed in a range of 4 to 4.5 V.

In the *RUSAL Company's* "Inert Anode Cell" project, electrolysis was carried out in medium- and low-temperature cryolite alumina melts (details on the electrolyte composition were not published) at a temperature range of 850-950°C [29]. In a 250-hour test in an 80-A cell with a vertical arrangement of a metal Cu-Ni-Fe anode and a wetted cathode, the voltage changed from 4 to 5.5 V during the first 100 hours and then remained stable. The contamination of aluminum with anode components was about 3.45%. The source [29] also indicated that a 5-kA cell with inert electrodes had been developed.

It is also important here to mention the low-temperature electrolysis in slurry electrolytes developed at *Brooks Rand, Ltd.* [12–14, 30, 31]. The electrolysis process in eutectic NaF-AlF₃ or KF-AlF₃ (with 4 wt% LiF) containing an excess of alumina was carried out at different anode and cathode current densities at a temperature of 750°C. One source [31] noted that the results were not as good as expected, since gray or black deposits covered the TiB₂ or TiB₂-C cathodes. The degree of deposits diminished with lower current density and at temperatures higher than 800°C. A recent source [30] mentioned that electrolysis tests in the KF-AlF₃ (or KF-AlF₃ and NaF-AlF₃ mixtures) electrolytes with durations up to 300 hours were carried out successfully at a temperature range of 700–850°C. The cells (10 and 300 A) were fitted with a Cu-Fe-Ni anode and TiB₂ cathode. A current efficiency of up to 99.5% and an aluminum purity of up to 99.5% were reported.

We can conclude from the research described that the new low-temperature aluminum production technology has potential. However, most of the studies suggest that aluminum electrolysis in potassium-cryolite-based electrolytes is more viable with an increase in either the temperature (above 800°C) or cryolite ratio (CR of >1.5). The NaF issue was bypassed by elevating the amount of NaF in the potassium cryolite. Unfortunately, this modification of the electrolyte required a significant increase in the operating temperature (compared with the concept proposed by Argonne). We also realize that low-temperature electrolysis assisted with the cathode behavior. The difficulties encountered during aluminum electrolysis in the potassium-cryolite-based electrolytes (CR of 1.3) at 700-750°C can be explained by the researchers' poor knowledge either about the fundamental properties of the molten KF-AlF₃ and KF-NaF-AlF₃ mixtures or about the distinctive features of low-temperature electrolysis.

Studies of the fundamental properties of the potassium-cryolite-based electrolytes intensified during the past years at the following research centers:

- *Argonne National Laboratory, Argonne, Illinois:* alumina solubility [7]
- *Institute of High Temperature Electrochemistry, Yekaterinburg, Russia:* electrical conductivity, liquidus temperatures, alumina solubility, impacts of additives (LiF, CaF₂) [11, 32-37]; IHTE in collaboration with RUSAL [11, 34]
- *Central South University, Changsha, China:* electrical conductivity, liquidus temperatures, surface tension, density [38–41]
- *Norwegian University of Science and Technology (NTNU), Trondheim, Norway:* electrical conductivity, alumina solubility [5, 7]

- *Slovak University of Technology, Bratislava, Slovakia (in collaboration with NTNU):*
phase diagram, density, viscosity, surface tension [42–45]

2.5 GOALS AND OBJECTIVES

This project is a continuation of the effort to develop a transformational process for the production of aluminum. The primary goal of the project is to resolve issues related to NaF buildup in the cells, which was identified in the previous DOE project as a potential “show-stopper.” The secondary goal is to demonstrate sustained cell operation in long-term tests in a 100-A cell. The third goal is to develop a design for a larger-scale 1,000-A cell.

3 RESULTS AND DISCUSSION

3.1 EXPERIMENTAL WORK

The experimental work was performed in the following tests:

- Aluminum electrolysis in a 20-A cell

The objectives of testing were to:

- Determine the operating window for low-temperature electrolysis in a laboratory-scale cell;
- Study the impacts of NaF on the electrolysis process;
- Distinguish cathode encrustation issue;
- Identify voltage anomalies;
- Analyze the electrolyte composition and establish how it changes during electrolysis;
- Develop an alumina feeding strategy; and
- Track the impurity level of the metal product during electrolysis.

- Aluminum electrolysis in a 100-A cell

The objectives of testing were to:

- Confirm cell operation in long-term tests and
- Determine long-term materials compatibility.

- Aluminum electrolysis in a 1,000-A cell

The objective of testing was to:

- Demonstrate cell operation at a semi-industrial scale.

All electrolysis tests were performed in a cell vertically fitted with an aluminum bronze anode and two wetted cathodes in the KF-AlF_3 or $\text{KF-AlF}_3\text{-NaF}$ (2–4 wt%) electrolytes with a CR of 1.3 at a temperature range of 700–770°C. Typically, the anode current density was 0.45 A/cm^2 , and the cathode current density 0.52 A/cm^2 .

3.1.1 Setup for 20-A and 100-A Cells

An electrolytic cell with a vertical electrode orientation was designed. The 20-A electrolysis cell and the 100-A cell had the same configuration. The experimental setup is shown in Figures 1–4. The crucible containing preweighed salts was placed into the alumina furnace tube and sealed with a metal cap. An anode was made of commercially available aluminum bronze (C630) with a composition of Cu, Al, Ni, Fe, and Mn at 80.5, 10.2, 4.9, 3.2, and 1.0%, determined by scanning electron microscopy-energy dispersive spectroscopy (SEM-EDS) analysis. Typically, one plate anode and two plate cathodes were used in a test. The anode size was 7.0 x 3.2 x 1.3 cm for the 20-A cell and 13.0 x 8.6 x 2.5 cm for the 100-A cell. The ACD was about 2 cm. The electrodes were completely immersed in the molten electrolyte and suspended by leads encased in alumina tubes. The leads were threaded into the electrodes to ensure reliable electrical contact. A DC power supply (TDK-Lambda GENESYS™ 40-250) provided a constant electrical current during electrolysis.

To make the melt temperature profile more uniform, a stainless-steel shell inside the furnace was used to house the alumina furnace tube. A round-bottom crucible with the electrolyte was placed into the alumina furnace tube and then closed with a water-cooled metal cap. The metal cap had ports sealed with compression tube fittings to support the electrodes. It also featured an alumina feeding tube, a silicon carbide or alumina case for the thermocouple, alumina tubes for gas inlet and outlet, and a pressure gauge. Nitrogen gas was delivered to the cell through a Teflon tube. A pressure release valve was fixed to the inlet gas tube just before the cell and was set at 1.5 pounds per square inch (psi) above atmospheric pressure to prevent overpressurization of the cell. In some experiments, argon gas was used instead of nitrogen.

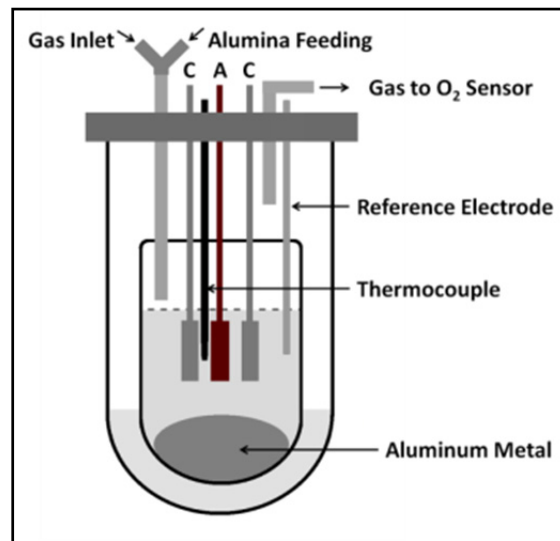


Figure 1 Schematic of experimental cell

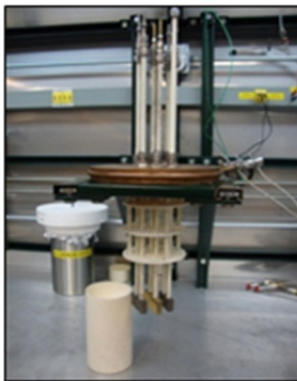


Figure 2
20-A experimental setup
with two wetted
cathodes and one
aluminum bronze anode

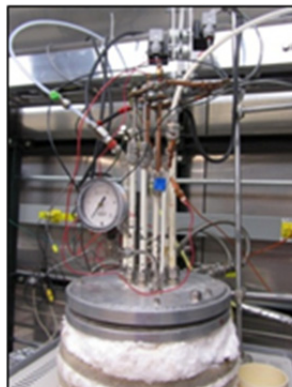


Figure 3 Top view of
assembled water-
cooled furnace-tube
end-cap



Figure 4 Experimental facility
(Furnace with assembled electrolysis
cell positioned under the exhaust
hood, two racks with oxygen
sensors, furnace temperature
controllers, power supplies, and
computers that served two
experimental setups)

Oxygen gas generated at the anode was flushed out by the inert gas in the cell. Before the outlet gas was analyzed for its oxygen content, it was passed through a glass wool filter, a container with a sodium hydroxide solution, and a column with desiccant. A sketch of the outlet gas scrubber system is shown in Figure 5. The oxygen sensor (Cambridge Sensotec Ltd. Rapidox 2000 oxygen analyzer) was calibrated with two nitrogen-oxygen gas mixtures containing 0.5% and 10% oxygen. The nitrogen gas flow rate into the furnace was regulated with a flow meter and maintained at 1.1 L/min, as recommended by the Rapidox gas analyzer.

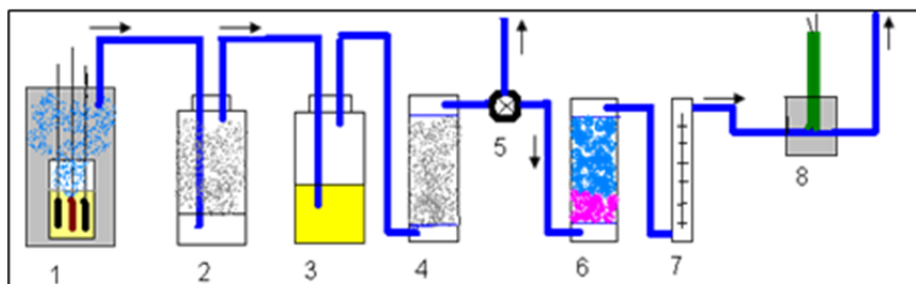


Figure 5 Sketch of the outlet gas scrubber system (1 is furnace with electrolytic cell; 2 is scrubber with quartz wool; 3 is bottle with NaOH; 4 is column with quartz wool; 5 is valve; 6 is desiccant; 7 is flow meter; 8 is oxygen sensor.)

For electrolysis testing, the electrodes were lowered into the melt and then energized. After electrolysis, the electrodes were removed from the melt prior to electrolyte solidification.

An automatic feeding system was developed to deliver desired amounts of alumina at specified intervals. Timing was adjusted so that the alumina feeding rate would be the same as the alumina consumption rate. During electrolysis, the cell temperature decreased slightly (by 0.3 to 0.5°C) when alumina was added, even if the addition was small (about 0.7 g). This temperature variation helped to verify that the automatic feeding continued without interruption throughout the experiment.

The data on cell voltage, current, operating temperature, and cathode and anode potential were monitored by a National Instruments data acquisition unit and recorded once every second by the LabVIEW computer program. The oxygen content of the outlet gas was recorded every 30 seconds by using the Rapidox software.

3.1.1.1 Electrical leads

Aluminum bronze rods were used as the material for the anode electrical leads in the 20-A tests. Since the size of C630 alloy rods needed for 100-A tests was not available, a special test was performed to choose appropriate materials for the anode electrical leads to be stable in the potassium cryolite melt at electrolysis conditions. The copper and copper alloys C655, C642, and C630 were tested and compared in one experiment. These materials, in the shape of a rod, were used as anodes in the KF-AlF₃ electrolyte (CR of 1.3) at temperature and current density ranges of 700–750°C and 0.4–0.6 A/cm². The rods were not shielded with alumina cases, and the electrolysis cell was not sealed. The C642 alloy was completely destroyed by 2.5 hours of electrolysis. The other materials were in good shape after 5 hours of electrolysis and were

covered with a thick black oxide layer. The C642 bronze alloy and copper were determined to be applicable materials for use as electrical leads to the aluminum bronze anode.

3.1.1.2 Reference electrode

The electrolysis cell was equipped with two molybdenum quasi-reference electrodes to help identify the origin and extent of voltage anomalies. The potential between the reference electrode and the anode (E_A) and the potential between the reference electrode and the cathode (E_C) were monitored during electrolysis. Platinum, tungsten, and molybdenum were tested as candidates for the quasi-reference electrode. Molybdenum was chosen because of its stability in molten fluorides and its low cost. Sometimes, especially during long-duration testing, Mo electrodes were replaced with new electrodes. This typically did not cause any appreciable changes to the potential readings.

3.1.1.3 Sample analysis

Before, during, and after electrolysis, samples of electrolyte were collected by freezing the electrolyte on an alumina rod or by suctioning it into an alumina tube. Concentrations of aluminum, potassium, sodium, and possible impurities in the electrolyte were determined by inductively coupled plasma-optical emission spectrometry (ICP-OES). The oxygen content in the electrolyte samples was analyzed by a LECO RO600 oxygen determinator.

Impurities in the produced aluminum metal caused by the anode corrosion were also determined by ICP-OES and ICP-mass spectrometry (MS). The composition of the anode scale was analyzed by Bruker D8 ADVANCE x-ray diffraction (XRD) and SEM-EDS. In a series of experiments, an aluminum metal heel was added to the cell before electrolysis to allow aluminum samples to be taken during the early stages of electrolysis.

3.1.2 Electrolyte

3.1.2.1 Composition

Potassium fluoride (Aldrich) with a purity of 99% was used for the experiments. The alumina and aluminum fluoride were supplied by Noranda Aluminum Smelter. The electrolyte was composed from KF (47.35 wt%) and AlF_3 (52.65 wt%) in a molar ratio corresponding to a CR of 1.3. In some tests, KF (Aldrich) was added, but the CR was maintained at 1.3, where it was calculated as $CR = (N_{KF} + N_{NaF})/N_{AlF_3}$. About 1.5 kg and 6.0 kg of electrolyte were used for the 20-A and 100-A tests, respectively.

Before electrolysis testing was performed, the alumina powder was dried at 400°C for 4 to 6 hours and then kept in the thermo cabinet.

3.1.2.2 Impurities introduced with raw chemicals

Oxygen-containing impurities. The alumina and AlF_3 supplied by Noranda Aluminum Smelter were analyzed for impurities by using ICP and LECO methods. The alumina was found to contain about 0.3 wt% of sodium, and the AlF_3 contained about 4.5 wt% of alumina and about 0.6 wt% of other oxide-impurities. Information on the impurities in alumina and AlF_3 is presented in Tables 1 and 2.

Table 1 Content of impurities, excluding alumina, in aluminum fluoride (wt%)

Source	Na ₂ O	CaO	Fe ₂ O ₃	SiO ₂	SO ₃	Total
Argonne data from 2010	0.26 (Na 0.19)	0.024 (Ca 0.018)	0.014	0.216 (Si 0.1)	0.097	0.612
Noranda data from 2010	0.32	0.021	0.007	0.25	0.06	0.658

Table 2 Content of impurities in alumina (wt%)

Source	Na	Ca	Cr	Fe	Mn	Mg	K	Si	Ti	V	Zn	LOI	Ni	Ga
Argonne data from 2010	0.16	0.01	<0.003	<0.003	<0.003	<0.003	<0.003	<0.003	<0.003	<0.003	<0.003	1.90	n.d. ^a	n.d.
Noranda data from 2007	0.31	0.028	n.d.	0.004	0.0005	n.d.	n.d.	0.004	0.0003	0.0002	0.007	0.8	0.0007	0.005

^a n.d. = not determined.

KF (Aldrich) with a purity of 99% was used for the experiments. Since KF is very hygroscopic, it was delivered from the supplier in small batches and stored in a dry cabinet. The oxygen content in KF was determined before each experiment and contained less than 0.3 wt% oxygen.

Samples of the electrolyte were taken before electrolysis began and again before any aluminum was added to the melt. The oxygen content in these samples was then determined to get a preliminary estimate of the amount of alumina present. In general, the amount of oxygen in the electrolyte was about 2.5–2.7 wt% just after melting. The oxygen could have been introduced into the melt from the moisture in the KF and from the oxygen-containing impurities in the AlF₃, the main component of which is an aluminum oxide.

The concentration of oxygen (in volume percent [vol%]) in the outlet gas flow detected at the beginning of electrolysis is shown in Figure 6. It was observed that the highest level of oxygen present in the exit gas stream occurred during the first 60 minutes of electrolysis. Typically, the maximum concentrations observed were 4.5–5.0 vol%. The amount of oxygen that evolved from the melt during this time period was calculated to be about 1–2 vol%. It was concluded that this elevated level of oxygen in the outlet gas flow was due to the purification of the oxygen-containing impurities in the electrolyte during this early stage of electrolysis.

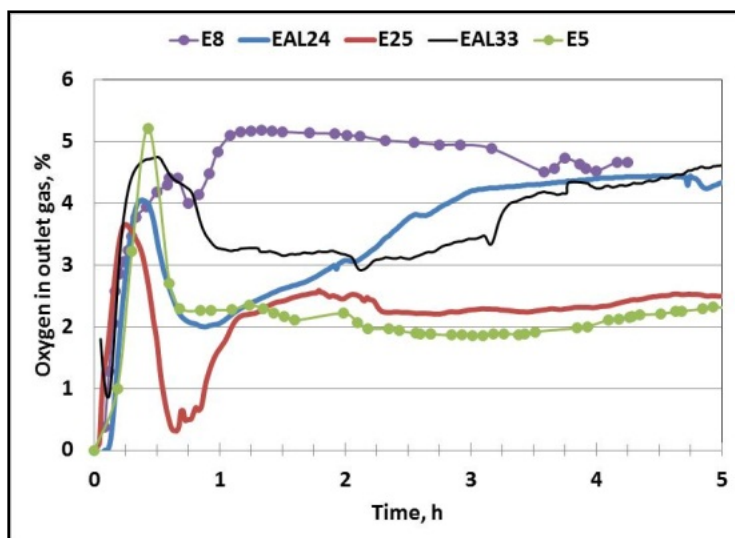


Figure 6 Oxygen in outgas flow during first hours of electrolysis for KF-AlF_3 at 700°C (Experiments E8, EAL24, E25, EAL33) and for $\text{KF-AlF}_3 + \text{NaF}$ (2 wt%) at 730°C (Experiment E5)

Silicon impurity. Silicon is introduced into the electrolyte mostly as an impurity of AlF_3 . It was assumed, according to the ICP analysis of AlF_3 , that the concentration of silicon in the KF-AlF_3 with a CR of 1.3 should not exceed 0.1 wt%. In our experiments, silicon could also be introduced to the cell together with Thermeez alumina putty, which has been used on occasion to attach the alumina current lead shields to the top of electrodes. The Thermeez alumina putty is composed of high-purity alumina bonded with a ceramic; the ceramic likely contains silica. The content of silicon in the electrolyte during 100-A electrolysis (Experiments 100E37 and 100E41) at 750°C is shown in Figure 7. In spite of obvious data variations, the average silicon concentration in both experiments is 0.5 wt%. Since the silicon concentration does not decrease with time, it can be assumed that silicon is not reduced during low-temperature electrolysis in potassium-cryolite-based electrolytes. It is known [2] that silica can partially react with cryolite or aluminum fluoride (AlF_3), forming silicon tetrafluoride (SiF_4), in an open system. But the rate of this reaction, even at $1,000^\circ\text{C}$ in sodium cryolite (Na_3AlF_6), is very low. The solubility of silica (SiO_2) in sodium cryolite is about 5 wt% at $1,000^\circ\text{C}$. Apparently, it is significantly lower at $700\text{--}750^\circ\text{C}$, and, under the conditions of our experiments, the SiO_2 is probably not soluble. The presence of the solid silica particles, which were not uniformly spread in the electrolyte, can explain the variation in the ICP data.

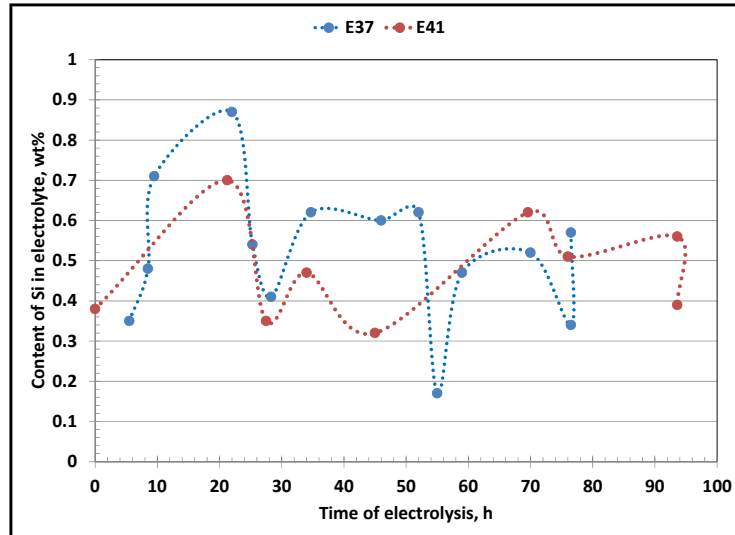


Figure 7 Content of silicon in KF-AlF₃ electrolyte in 100-A electrolysis at 750°C (Experiments 100E37 and 100E41)

Sodium impurity. The alumina supplied by Noranda Aluminum Smelter was analyzed for sodium impurities by using the ICP-OES. The alumina contained about 0.3 wt% of sodium. Under laboratory-scale conditions (20-A and 100-A cells), the content of sodium in the KF-AlF₃ melt remained constant throughout the 56 hours in a 20-A cell (Figure 8, Experiment E6) or throughout the 96 hours in a 100-A cell (Figure 9). The measured and calculated sodium concentrations in potassium cryolite containing 2 wt% NaF (Figure 8, Experiments E5 and EAL19) are stable and in accordance with each other.

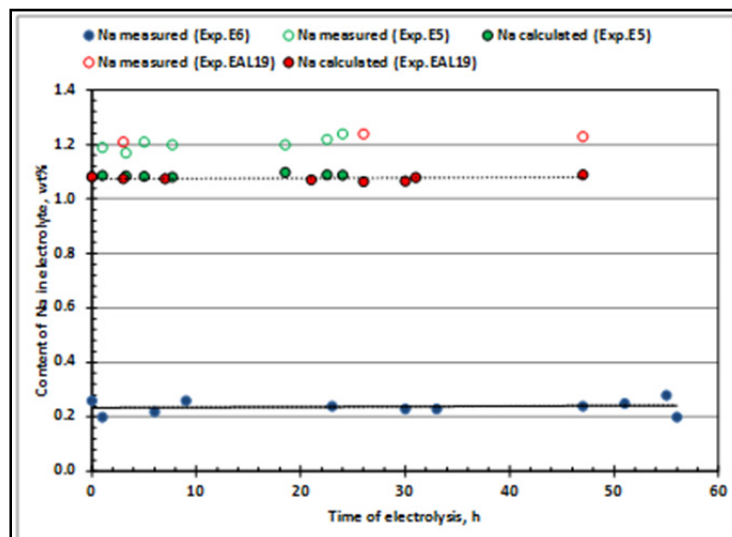


Figure 8 Measured and calculated sodium concentrations during 20-A electrolysis in KF-AlF₃ at 700°C (Experiment E6) and in KF-AlF₃ + NaF (2 wt%) at 700°C (Experiment E5) and at 750°C (Experiment EAL19)

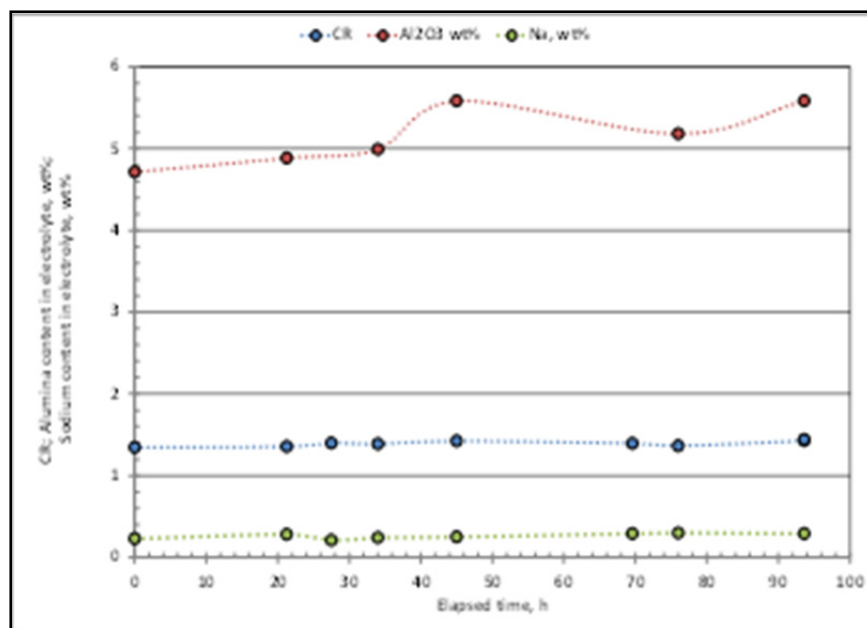


Figure 9 Measured CR and concentration of alumina and sodium in electrolyte during 100-A electrolysis in KF-AlF₃ at 750°C (Experiment 100E41)

Impurities introduced by anode corrosion. Electrolyte samples taken during electrolysis were analyzed for the presence of impurities caused by the corrosion of the anode. The amount of Cu, Fe, Ni, and Mn was less than 0.05 wt% throughout the entire test.

Cryolite ratio. In order to trace the change of the electrolyte CR during electrolysis in 20-A tests, the K, Al, and O contents in the electrolyte samples were analyzed. It was assumed that the Al element was present in the electrolyte as AlF₃ and Al₂O₃. The measured values of concentrations were compared with calculated ones. For calculations, the amount of added and consumed alumina at the time of each sampling session was taken into account. Figure 10 shows that while the measured and calculated concentrations of KF remain close to each other, the measured content of AlF₃ is less than theoretically expected. Nevertheless, the molar ratio of potassium and AlF₃ concentrations in the electrolyte, even after 56 hours of electrolysis (Figure 11), does not change significantly and coincides within 5%. The change in the CR in the 100-A tests during 100 hours of electrolysis was also insignificant (Figure 9).

In order to maintain the electrolyte CR of 1.3, the amount of AlF₃ added to the salt mixture was increased appropriately.

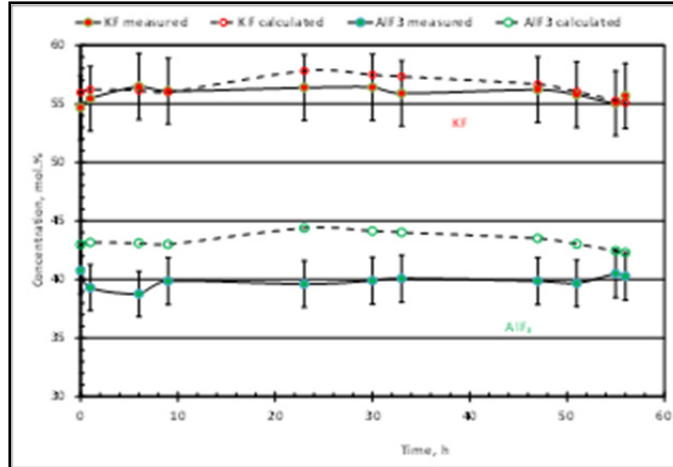


Figure 10 Measured and calculated concentrations of AlF_3 and KF during electrolysis in electrolyte KF-AlF_3 , CR of 1.37, at 700°C (Experiment E6)

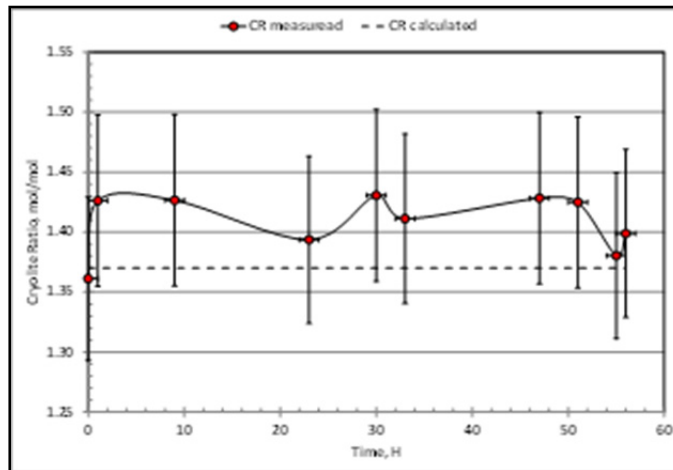


Figure 11 Measured and calculated CR in electrolyte KF-AlF_3 , CR of 1.37, at 700°C (Experiment E6)

Alumina concentration. The alumina concentration in the electrolyte was checked throughout each experiment. The alumina content in the electrolytes being studied over all composition and temperature ranges was found to be close to saturation and stabilized near 4.5 to 5.5 wt% (Figure 12). Over the range of test conditions, the effect of temperature and composition on alumina solubility was observed. An increase of 30°C changed the alumina concentration in the electrolyte KF-AlF_3 (CR of 1.3) from 4.4 to 5.4 wt%, on average (Figure 12, Experiments E-29 and E-26). An increase in the NaF concentration at a constant temperature decreased the solubility of the alumina (Figure 12, Experiments EAL-19 and E-9). A change in the CR from 1.3 to 1.1 sharply decreased the solubility of the alumina (Figure 12, Experiment EAL-14).

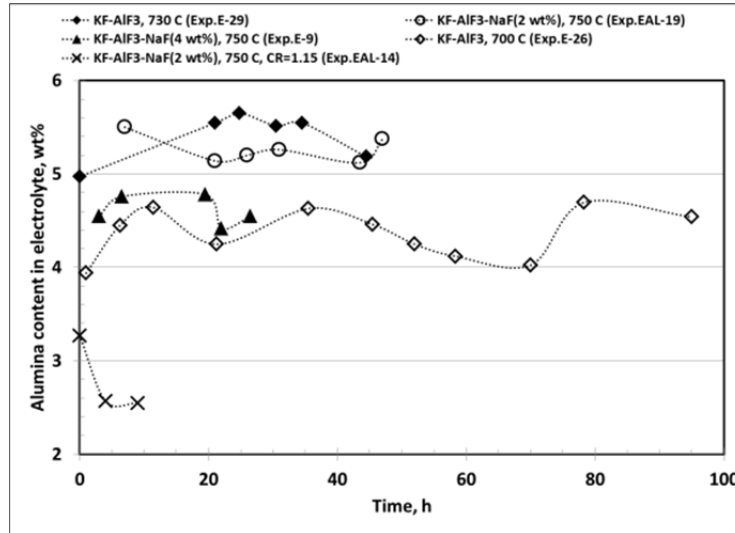


Figure 12 Alumina content in the electrolytes during 20-A electrolysis

Electrolyte constitution. Even though no significant amount of evaporation was observed during electrolysis at 700°C, the amount of electrolyte evaporation did increase as the temperature increased. The white substance that condensed on cold parts of the electrolytic cell was analyzed by SEM-EDS, and the condensate was found to consist of potassium aluminum tetrafluoride (KAlF₄). The same finding was made when the crystals covering the anode surface were analyzed. The optical image of the surface showing the translucent crystals covering the anode surface and the SEM image of surface crystals and its corresponding EDS spectrum are presented in Figure 13. The SEM analysis confirmed that the main component of the potassium cryolite, with a low molar ratio, is KAlF₄.

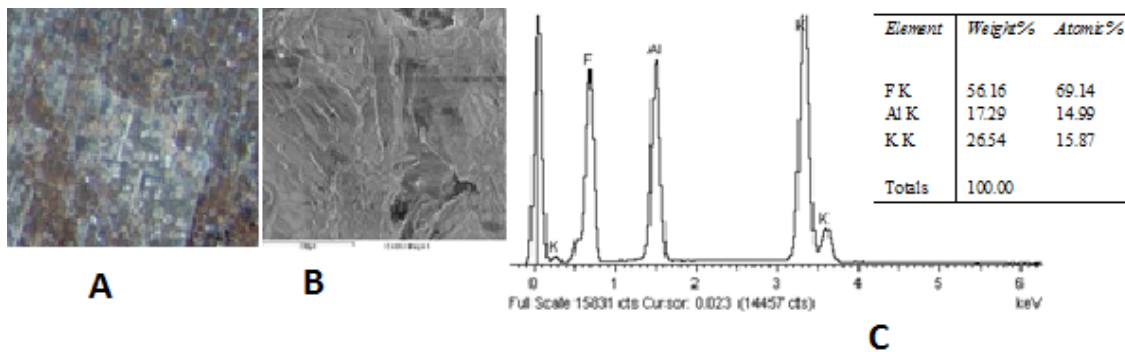


Figure 13 Optical image of the surface showing the translucent crystals covering the anode surface (A); SEM image of surface crystals (B); and graph of corresponding EDS spectrum (C)

Liquidus temperature. Additions of NaF to the KF-AlF₃ melt, with a molar ratio of N_{KF}/N_{AlF_3} being less than 1.7, significantly increased the temperature of the primary crystallization. To establish the liquidus temperature of the electrolytes being studied, the liquidus was measured in the test cell at the beginning and/or after electrolysis by recording the electrolyte

temperature during cooling. Note that the technique of liquidus measurement in an electrolysis cell was tested by using a sodium chloride (NaCl) melt. The molten point of NaCl was found to be 801°C, which coincides very well with the reference data. It can serve as the proof of competency of similar measurements of temperature under the experimental conditions. Liquidus temperatures measured in the electrolysis cell are listed in Table 3. To determine their alumina content, the electrolyte samples were taken before electrolysis at temperatures between 730 and 750°C. The liquidus temperatures that were determined were in line with the published data (Figure 14). The values of liquidus obtained in Experiment E5 before and after electrolysis were similar. Thus there is evidence that the electrolyte composition did not change significantly during the test.

Table 3 Liquidus temperatures of electrolytes measured in the electrolysis cell

Experiment	Electrolyte	CR	T _{liq} (°C)	Comment
E4	KF-AlF ₃	1.4	643	After electrolysis
E5	KF-AlF ₃ + NaF(2 wt%)	1.4	705 699	Before electrolysis After electrolysis
E8	KF-AlF ₃	1.3	630	Before electrolysis
E7	KF-AlF ₃ + NaF(4wt%)	1.3	656	Before electrolysis
E9	KF-AlF ₃ + NaF(4wt%)	1.3	662	Before electrolysis
100E27	KF-AlF ₃	1.3	632	After electrolysis

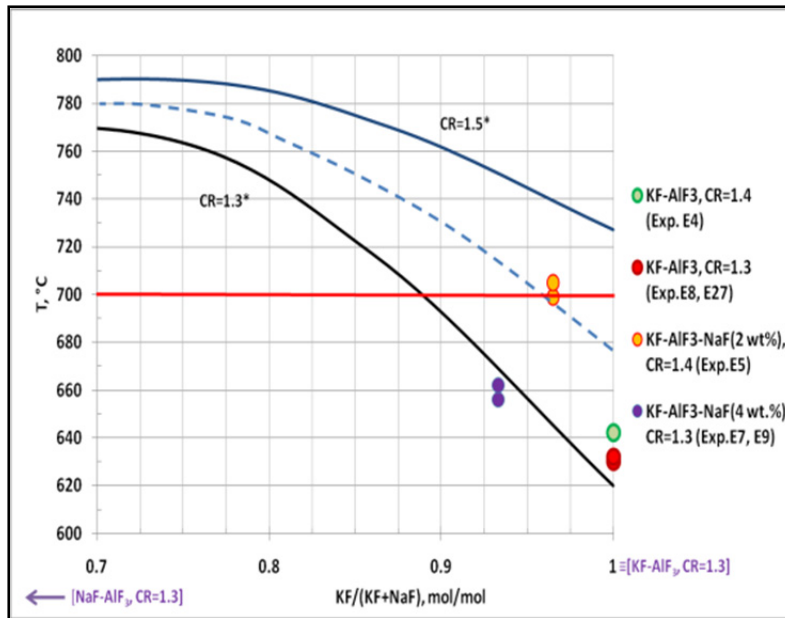


Figure 14 Liquidus temperatures of electrolyte, measured and available data [36]

3.2 20-A ELECTROLYSIS TESTING

3.2.1 Operating Parameters

A typical plot of electrolysis performed in the KF-AlF_3 electrolyte at 700°C is shown in Figure 15. The voltage was stable (3.55 V), with a maximum voltage oscillation of 0.02 V. The voltage oscillation during 1 hour of electrolysis from the 74th to the 75th hour is presented in Figure 16. The cathode and anode potentials did not change significantly. The oxygen level in the outlet gas stabilized at around 5%, thus confirming the smooth course of electrolysis. The alumina content in the electrolyte was 4.5 wt%, on average.

At the beginning of each test, the set temperature was manually adjusted to the desired value. Once adjusted, the set temperature was not altered so that the rise in temperature during the test could be determined. Under conditions when the electrolysis process was stable and

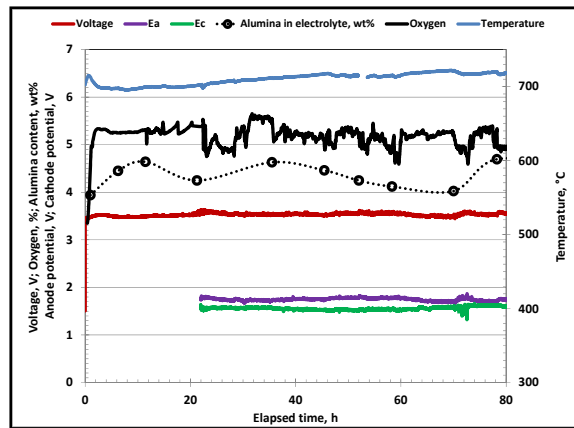


Figure 15 Operating parameters of 20-A electrolysis in KF-AlF_3 electrolyte (Experiment E26)

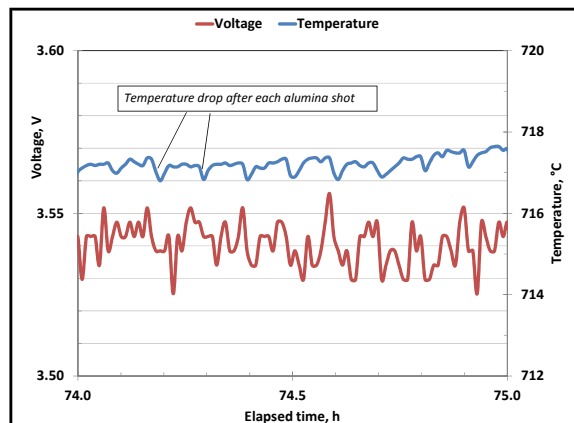


Figure 16 Enhanced plot of temperature change and voltage oscillation in 20-A electrolysis (Experiment E26)

consistent, an increase in the operating temperature decreased the cell voltage and enhanced the oxygen content in the outlet gas.

The operating parameters of electrolysis and descriptions of performed tests are presented in Appendix Table A-1. The voltage values in the 20-A tests were in a range of 3.3 to 3.8 V, with a maximum voltage oscillation of 20 mV. For comparison, a baseline test using the same cell design with vertical electrodes but fitted with a graphite anode and two graphite cathodes was performed. The plot of this electrolysis is given in Figure 17. At the beginning of electrolysis, the voltage was 3.0 V, but it increased to 4.0 V by the 17th hour. After electrolysis, the anode was completely consumed, as expected.

After each test, the aluminum bronze anode was covered by a thin, flaky, oxide scale. Pieces of this scale were always found on top of the frozen electrolyte, suggesting that the oxide layer began spalling after the electrodes were raised out of the melt. The aluminum bronze anodes after the 20-A test in KF-AlF₃ electrolyte are shown in Figure 18.

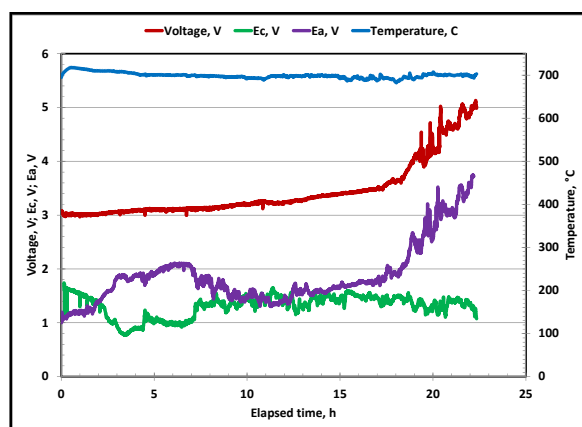


Figure 17 Electrolysis plot in a 20-A cell with vertical graphite anode and two graphite cathodes, in KF-AlF₃ electrolyte with a CR of 1.3

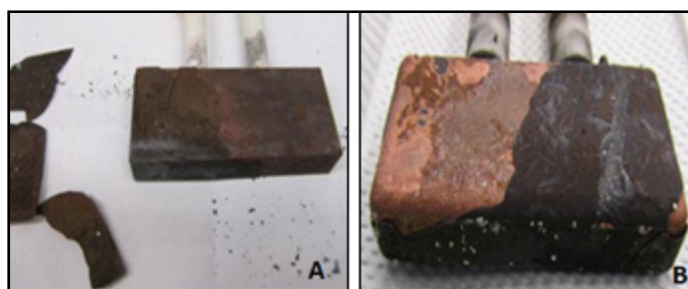


Figure 18 Aluminum bronze anode after 20-A electrolysis in KF-AlF₃ (Anode scale cracked and spalled after the electrodes were raised out of the electrolyte and cooled. Exposure was for 48 hours at 750°C for Experiment EAL12 and for 70 hours at 700°C for Experiment EAL25.)

3.2.2 Current Efficiency

The oxygen concentration in the outlet gas as measured by an oxygen sensor depends on the inert gas flow rate. For this reason, the gas flow rate and pressure in the cell were carefully controlled. At a nitrogen flow rate of 1.1 L/min, the current efficiency (CE) that was calculated according to the oxygen content detected in the outlet gas was in good agreement with the CE calculated on the basis of the mass of produced aluminum metal. The CE calculations for some experiments are compared in Table 4. The average and maximum values of CE based on the oxygen concentration in outlet gas are presented.

Table 4 Current efficiency based on the evolved oxygen and produced aluminum contents in 20-A tests

Exp. No.	Test Description and Conditions	CE Based on O (% , avg/max)	CE Based on A (%)	Al Expected (g)	Al Produced (g)
E8	KF-AlF ₃ , 700°C, 24 h	65/92	75	110	120
E9	KF-AlF ₃ -NaF(4 wt%), 750°C, 24 h	65/84	83	114	133
EAL11	KF-AlF ₃ , 700°C, 47 h	55/76	50	160	154
EAL12	KF-AlF ₃ , 750°C, 47 h	55/82	50	170	160
EAL26	KF-AlF ₃ , 700°C, 96 h	55/80	54	360	346
EAL45	KF-AlF ₃ , 750°C, 56 h	78/98	78	327	337

Actually, CE is not a critical parameter for laboratory-scale electrolysis because the construction and design of a small electrolytic cell often does not provide electrical and/or materials flow of sufficient quality. Nevertheless, it is still possible to trace the influence of process modifications on the CE value during laboratory-scale testing.

The maximum value of CE in a 20-A cell fitted with one aluminum bronze anode and two wetted cathodes at an anode current density (i_a) of 0.45 A/cm² and a cathode current density (i_c) of 0.52 A/cm² was 80–85%. The increase in current density resulted in a rise in the CE. In the electrolysis test presented in Figure 19, currents of 15, 20, and 25 A were applied. Both the amount of oxygen generated on the anode and, consequently, the CE rose with the increasing current density, as expected. At a current of 25 A ($i_a = 0.56$ A/cm² and $i_c = 0.65$ A/cm²), the CE reached 95%. The oxygen amount that evolved on the anode and was detected by the oxygen sensor promptly responded to changes in the operating parameters during electrolysis, such as in the temperature or current. Figure 19 shows that the oxygen concentration changed immediately following the change in the current.

Based on the value of CE calculated, in accordance with evolved oxygen, the amount of consumed alumina can be estimated directly during electrolysis. According to these calculations, the frequency of automatic alumina feeding was corrected during the test. Without this correction, undissolved alumina would collect on the bottom of the cell and would inhibit the formation of an adequate coalesced aluminum metal product. Moreover, it is also possible to estimate the amount of aluminum being produced at any time throughout electrolysis. This estimate was used to determine the amount of impurities accumulated in the aluminum metal produced at the time of each metal sampling.

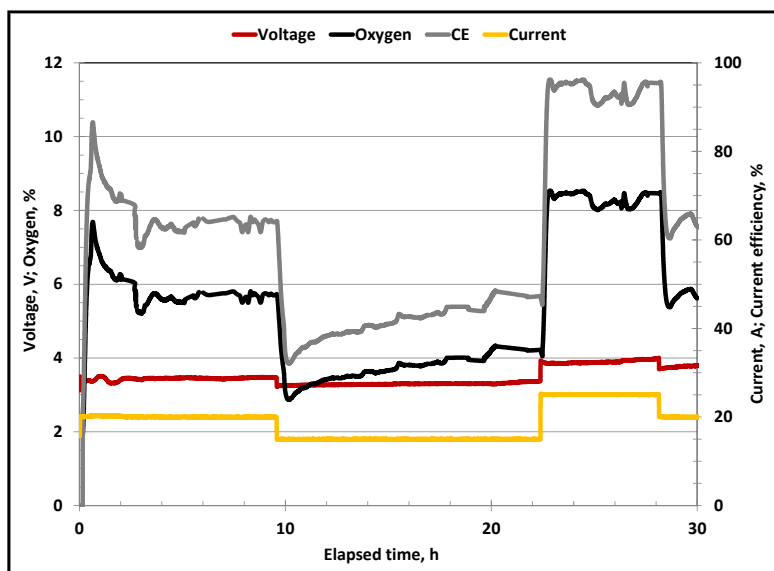


Figure 19 Current efficiency and operating parameters of electrolysis in KF-AlF₃ at 750°C (Experiment EAL31)

3.2.3 Voltage Anomalies

3.2.3.1 Effect of cathode and anode processes

The voltage deviations during aluminum electrolysis with an inert anode are determined mainly by the anode processes. The stable voltage and anode potential indicate a smooth and steady electrolysis. Nevertheless, a voltage instability cannot always be ascribed to the anode's behavior. To show an example of voltage anomalies, an electrolysis plot in the KF-AlF₃-NaF (4 wt%) electrolyte is presented in Figure 20. E_{cathode} and E_{anode} potentials can help determine which process has more impact on the cell voltage. During the first 2 hours, the voltage and E_{cathode} changes were similar, which indicates that the voltage anomalies could be attributed to the cathode process. An increase in temperature minimized the amplitude of the voltage oscillation. The oxygen formation stopped after the first hour of electrolysis and resumed after an increase in temperature.

Thus, using the quasi-reference electrode in a test with the KF-AlF₃-NaF electrolyte (4 wt%) further confirmed our understanding that the processes occurring on the cathode were also responsible for the voltage variation.

3.2.3.2 Cathode processes: NaF impact

According to the measured values of liquidus (Table 3), it seemed that even in spite of the presence of sodium in the potassium electrolyte with a low CR, there was still an opportunity to carry out electrolysis at 700°C in the potassium system with 2–4 wt% of NaF. Therefore, electrolysis in the KF-AlF₃ electrolyte containing 4 wt% of NaF was performed at 700°C. The plot of this test is shown in Figure 21. The voltage increased from 5.5 to 8.5 V by the fifth hour, and oxygen dropped below 2% by the first hour and decreased to near zero. Even interrupting the test, which was done to dissolve the oxide layer that formed on the anode and to refresh its surface, did not help the electrolysis improve. After the experiment was completed, a thick gray

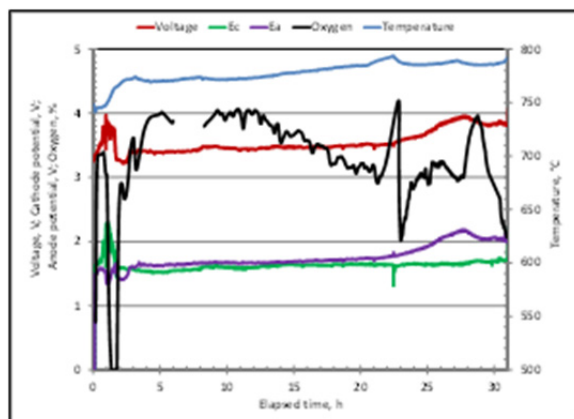


Figure 20 Effect of cathode and anode processes on voltage during electrolysis in KF-AlF₃-NaF (4 wt%) electrolyte (Experiment EAL21)

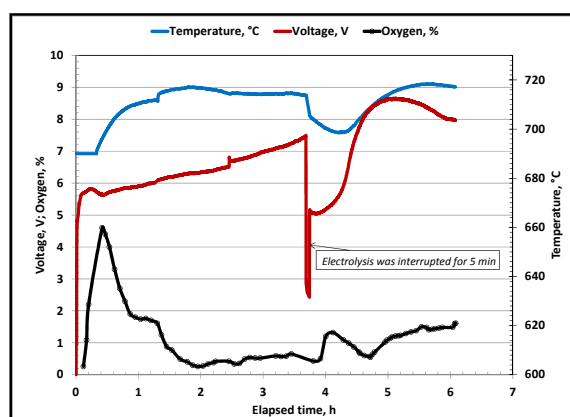


Figure 21 Plot of electrolysis in KF-AlF₃-NaF at 4 wt%, with a CR of 1.3 at 700°C (Experiment E7)

deposit covered the cathode, but the anode looked normal (Figure 22). The cathode deposit consisted of two layers (Figure 23). An internal layer, closer to the cathode's surface, was black and could be easily crushed. The external layer over the internal layer was gray, firm, and difficult to crush. In an XRD analysis of the milled cathode deposit (mixture of both layers), the material was determined to be KAlF₄ and K₃AlF₆. The XRD spectrum is presented in Figure 24. XRD analysis of the internal black layer (separated from the gray layer) detected only KAlF₄. The presence of K₃AlF₆ in the cathode deposit explains the solidification of the electrolyte on the cathode surface. No Al₂O₃ (as was reported in Source 31) was found.

A similar course of electrolysis during the first 2 hours was observed in Experiment E9 (Figure 25). However, after the temperature was increased to 750°C, the process recovered.

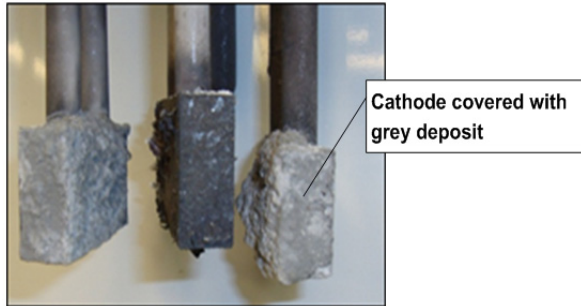


Figure 22 Electrodes after electrolysis in KF-AlF₃-NaF at 4 wt% at 700°C (Experiment E7)



Figure 23 Cathode deposit: gray external layer and black internal layer

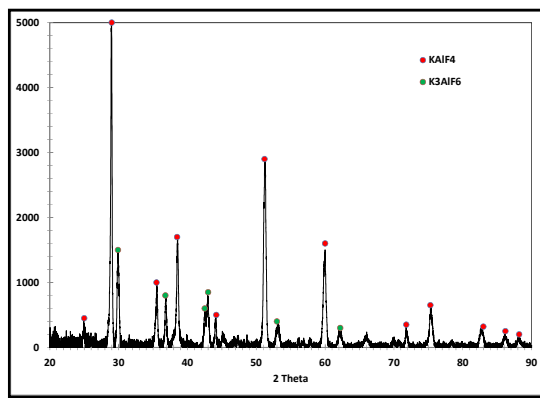


Figure 24 XRD spectrum of the cathode deposit (mixture of black and gray layers)

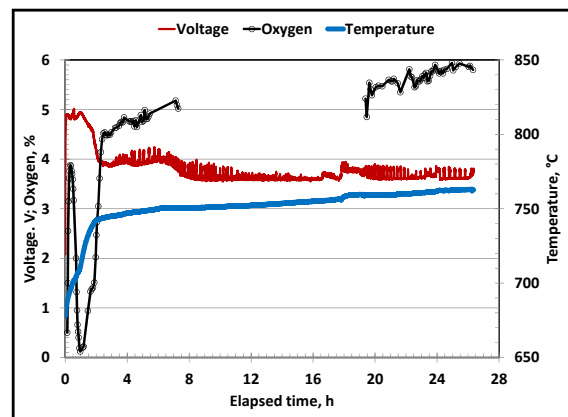


Figure 25 Plot of electrolysis in KF-AlF₃-NaF at 4 wt%, with a CR of 1.3 at 700 and 750°C (Experiment E9)

The oxygen evolution stopped after the first hour of electrolysis, and it resumed after an increase in temperature. The oxygen content in the outlet gas flow occasionally reached 6%. The voltage was around 3.6 V, but large voltage oscillations were observed. Despite this, the CE was observed to be 83%. The state of the electrodes after electrolysis in KF-AlF₃-NaF (4 wt%) at 750°C (Experiment E9) is shown in Figure 26.

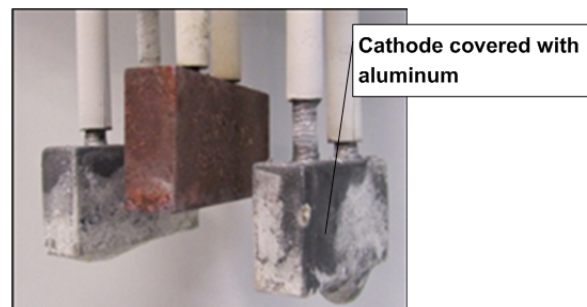


Figure 26 Electrodes after electrolysis in KF-AlF₃-NaF at 4 wt% at 750°C (Experiment E9)

The same course of electrolysis had been observed in the test with KF- AlF_3 -NaF (2 wt%) electrolyte (Experiment EAL19). A voltage oscillation with an amplitude of 250 mV occurred at 750°C at the beginning of electrolysis. This noticeable oscillation continued until the temperature was increased by 5–7°C. The enhanced plot of electrolysis between the 8th and 12th hour is shown in Figure 27. It can be seen that the voltage and temperature changes aligned with one another. It is possible to assume that the F^- content increased near the cathode surface as a result of aluminum depletion that led to the formation of K_3AlF_6 and to the shifting of the local electrolyte composition to the liquidus corresponding to the K_3AlF_6 crystallization. This caused the electrolyte to freeze on the cathode surface. The voltage increased and consequently the temperature increased as well. The rise in temperature initiated the dissolution of the cathode deposit and the renewal of the surface for the aluminum reduction.

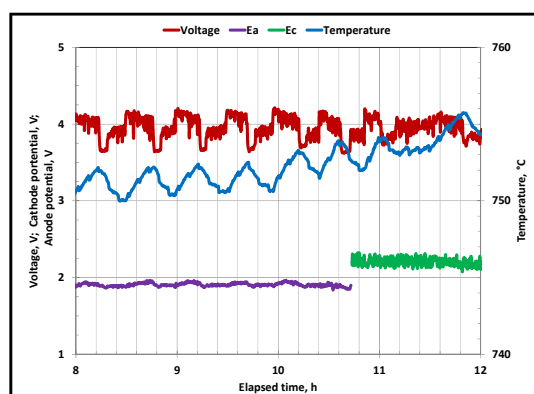


Figure 27 Enhanced plot of electrolysis in KF- AlF_3 -NaF (2 wt%) (Experiment EAL19)

It can be concluded that only the operating temperature needs to be adjusted to take the NaF content in the electrolyte into account. It is recommended that the minimal operating temperature for electrolysis in KF- AlF_3 -NaF electrolytes at 2 wt% and 4 wt% be as high as 750°C and 770°C, respectively.

These voltage anomalies caused by the cathode processes were first found in the low-temperature electrolysis in potassium cryolite with NaF additions. However, the same issue can arise at the beginning of low-temperature electrolysis in potassium electrolytes without NaF if the temperature of the electrolysis bath drops below 700°C when electrodes are being lowered into the melt.

3.2.3.3 Anode processes: corrosion, passivation

Note that in the majority of tests performed, no significant corrosion of the anode and no change in its geometrical size were observed. However, an example of a test (Experiment EAL32) that resulted in significant anode corrosion is shown in Figures 28 and 29. During 4–5 hours, the electrolysis stabilized (Figure 28) and the voltage increased very slowly. Furthermore, the cathode behavior affected the voltage instability, and the oxygen generation on the anode was suspended. A small increase in temperature seemed to recover the process. Figure 29 shows that after the 60th hour of electrolysis, the voltage began to continuously

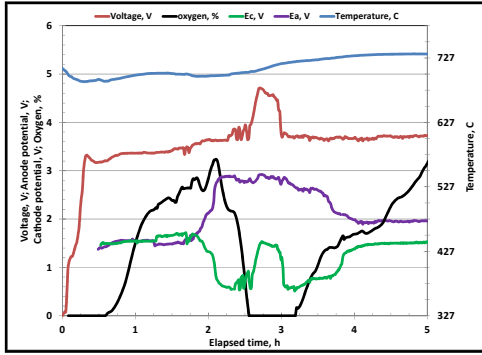


Figure 28 Parameters of electrolysis in KF-AlF₃ electrolyte during the first 5 hours (Experiment EAL32)

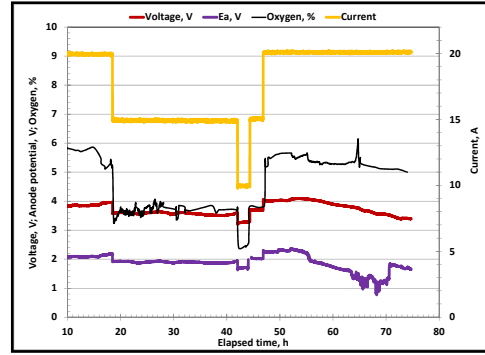


Figure 29 Decrease of voltage and anode potential values due to anode corrosion (Experiment EAL32)

decrease. The explanation for this was the evident corrosion of the anode, which was revealed after the test was stopped (Figure 30). The purpose of this experiment was to determine if a change in the current during the test could be a reason for anode corrosion. Nevertheless, it is quite possible that other inexplicable reasons, attributed specifically to this experiment, could have led to the destruction of the anode. This test shows that the voltage decrease can be attributed to the corrosion of the anode, if all other operating parameters are consistent.



Figure 30 Corroded anode after electrolysis in KF-AlF₃ electrolyte at 730°C (Experiment EAL32)

In contrast, cell voltage significantly increased in the case of anode passivation. In experiment EAL14 (Figure 31), the voltage and temperature rose continuously. By the 20th hour, the voltage had reached 8 V, and the temperature had risen by 40°C. The anode was covered by a dense but spongy-like scale that resulted in anode passivation (Figure 32). The formation of such a scale was explained by the bad quality of electrolyte, since it was discovered later that the KF used in this test contained about 30 wt% of moisture. When this was taken into account, the recalculated CR of electrolyte used in Experiment EAL14 was 1.1.

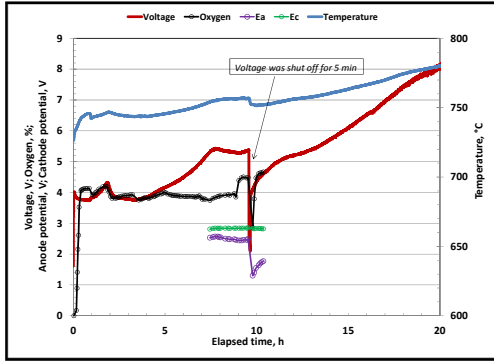


Figure 31 Voltage rise due to anode passivation during electrolysis in $\text{KF-AlF}_3\text{-NaF}$ (2 wt%) electrolyte (Electrolyte was moisturized, CR was about 1.1) (Experiment EAL14)



Figure 32 Anode covered with spongy-like scale after electrolysis in $\text{KF-AlF}_3\text{-NaF}$ (2 wt%) electrolyte at 750°C (Experiment EAL14)

3.2.3.4 Anode position in the electrolysis cell

It is very important to pay attention to the anode position in the electrolytic cell. If the anode is placed too deeply into the electrolyte, the aluminum metal can intermittently contact the anode. Brief voltage drops can be seen occasionally on the plot of voltage versus time (Figure 33). These indicate that the anode contacted the aluminum mass positioned at the bottom of the crucible. Half of the anode was dissolved in aluminum (Figure 34). The anode was lowered deeply into the cell in order to increase the alumina dissolution rate by gas bubbling. It was believed that the aluminum mass at the bottom of the cell would be flat, but instead it was more spherical or globular (Figure 35).

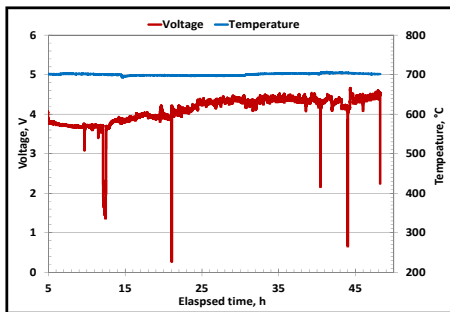


Figure 33 Voltage drops, which indicate the contact of the anode with aluminum metal (Experiment EAL10)



Figure 34 Half of the anode dissolved in aluminum metal (Experiment EAL10)



Figure 35 Aluminum produced in Experiment EAL10

On the other hand, if the anode was not completely immersed in the electrolyte, the voltage slowly increased and fluctuated. An example of such a test is shown in Figure 36. The portion of the anode that was not immersed was covered by an oxide layer that looked different than the anode oxide scale that had formed on the anode surface in the electrolyte (Figure 37). The

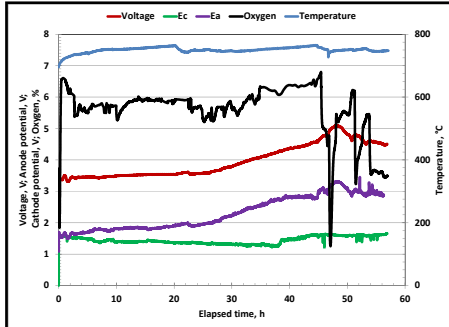


Figure 36 Plot of electrolysis in KF-AIF₃ electrolyte at 750°C (Anode plate was only partly immersed in the electrolyte) (Experiment E36)



Figure 37 Anode after electrolysis in Experiment E36 (Anode plate was only partly immersed in the electrolyte.)

immersed portion of the anode was covered with an uneven, nonuniform oxide layer that looked different than the anode oxide scale formed during steady electrolysis (see Figure 18). It is possible that the increase in current density, because of the decrease in anode working surface area, led to the formation of a denser, thicker layer, which, in turn, resulted in a voltage rise. It is also possible that the level of electrolyte was not flat near the anode due to the vigorous gas evolution, which can also affect the voltage fluctuation. The process was also complicated by the fact that the non-immersed parts of the electrodes were gradually covered by alumina. This led to the formation of a crust on the electrode that eventually impeded the oxygen evolution on the anode. In all probability, this phenomenon was specific only to electrode plates that were partially elevated above the electrolyte surface due to the large interface, and it was not appreciably noticeable where the electrode support rods rose above the electrolyte surface.

3.2.4 State of the Anode Surface before Electrolysis

The surface of the aluminum bronze anode was not specially treated or oxidized in advanced testing. Nevertheless, it was observed during numerous experiments that the state of the anode's surface before electrolysis affected the course of electrolysis. The anode was subjected to high temperatures and electrolyte vapors while suspended above the melt prior to electrolysis, in a cell filled with nitrogen. This resulted in the formation of a surface scale, and it affected the voltage values during electrolysis, the CE, and the amount of impurities in the aluminum produced.

Results of some tests, arranged in groups, are presented in Table 5. All tests were performed at an i_c of 0.52 A/cm^2 and an i_a of 0.45 A/cm^2 . Typically, the voltage was established during the first hour of electrolysis and remained constant for at least the next 24 hours. Therefore, the voltage values during the first 24 hours are comparable to those found in Table 3, despite the different test durations. The amount of copper that accumulated in the aluminum metal during first the 24 hours of electrolysis is also indicated in Table 5. The CE is presented as an average value calculated from the oxygen concentration in the outlet gas (CE_{Ox}) and as a value obtained from the produced aluminum mass (CE_{Al}).

Table 5 Parameters for 20-A electrolysis testing

Group No. and Conditions for Anodes Suspended over Melt before Electrolysis	Exp. No.	NaF (wt%)	T (°C)	Voltage during First 24 Hours (V)	Test Duration (h)	CE _{Ox} /CE _{Al} (%)	Copper in Produced Aluminum by 24th Hour (wt%)	Copper in Produced Aluminum (wt%)
I 900°C 1 hour	E3	2	700	4.75	10	^a /30	1.5	^a
	E4		700	4.87	24	^a /40		1.5
	E5		730	4.61	24	^a /40		3.5
	E6		700	4.75	56	35/40		4.4
II 750°C 2 hours	EAL11		700	3.60	48	55/50	0.72	0.9
	EAL24		700	3.31	32	62/66	0.3	0.3
	E25		700	3.60	70	51/57		0.5
	E26		700	3.55	80	55/54		0.7
	E29		700	3.47	30	60/64		0.8
	E30		700	3.67	62	62/ ^b		1.8
III 750°C 2 hours	EAL12	2	750	3.41	48	55/50	0.35	0.4
	EAL38		750	3.38	46	62/60	0.15	0.15
	EAL17		750	3.42	11	50/50		0.4
	EAL19		750	3.42	56	62/67	0.94	0.9
	E9		4	750	3.5	24	65/80	0.8
IV 750°C Surface protected from contact with vapors	EAL44 ($i_a = 0.4A/cm^2$)		750	3.33	51	72/80	0.10	0.4
	EAL43 ($i_a = 0.5A/cm^2$) ^c		750	3.46	76	50/60	0.3	0.65
	EAL45 ($i_a = 0.6 A/cm^2$)		750	3.60	56	78/78	0.42	0.4
^a Not measured. ^b The weight of the aluminum was not measured, because the anode fell into the melt due to the destruction of the electrical leads. ^c The current density i was 0.5 A/cm ² only during the first 24 hours, then it was increased to 0.63 A/cm ² .								

Group I unites tests in which electrodes were suspended over the electrolyte while the temperature in the cell reached 900°C. Such a high temperature was necessary because in these tests, chemicals for the electrolyte were melted directly in the cell before electrolysis. The average voltage ranged from 4.6 to 4.9 V at 700°C. These tests are characterized by the rather low CE (about 40%) and raised copper content in the produced aluminum (1.5–4.4%).

Group II electrolysis tests were conducted at 700°C. The electrodes were held above the melt at a temperature no higher than 750°C during the 1 to 2 hours prior to electrolysis. This was possible because the method of electrolyte preparation was updated or because pre-prepared electrolyte was used. The typical voltage value in these experiments was near 3.6 V at 700°C, which is about 1 V below the voltage values of tests from Group I. The CE reached 60%, and the copper impurities in aluminum amounted to less than 1 wt%.

Group III combines tests performed at 750°C in electrolytes composed of only potassium cryolite or of potassium cryolite with the addition of NaF (2–4 wt%). The addition of NaF in such small amounts did not noticeably change the value of voltage. Hence, for this group of tests, the voltage was in a range of 3.4 to 3.5 V, which is 0.1 to 0.2 V lower than Group II voltage. The CE did not differ significantly from the CE of Group II, nor did the quality of produced aluminum.

In the Group IV tests, the anode surface was protected from contact with vapors while the electrodes were suspended over the melt. The three experiments from this group were carried out at different current density levels that affected the voltage value. Nevertheless, the voltage in Experiment EAL43 with an applied current density of 0.5 A/cm², CE, and copper concentration in aluminum resulted in the same range of values as those from the Group III tests.

To determine the composition of the scale that formed on the surface of the aluminum bronze anode before electrolysis, special tests were done while it was suspended in the upper part of the cell at heating. An aluminum bronze sample was fixed in an electrolysis cell above the melt and heated. The change in temperature was programmed to match the electrolysis tests from Group I or III (see Table 5). Sample N1 was sustained at a maximum temperature of 750°C for 2 hours, and sample N2 was sustained at 900°C for 1 hour. After testing, both samples were covered with a black scale (Figure 38 A). The scale on sample N1 was 0.02-mm thick and impossible to detach or scrub. The scale on Sample N2 was 0.13-mm thick. It was fragile, easily detachable, and brown on the side that faced the aluminum bronze (Figure 38 B).

XRD spectra of the black and brown sides of the scale from Sample N2 are shown in Figure 39. The brown side mainly indicated copper. The basic composition of the same flake on the black side was copper and oxides of all the metals that were constituents of the aluminum bronze, in their highest oxidation state: CuO, Al₂O₃, NiO₂, Ni₂O₃, Fe₃O₄, and Mn₃O₄. Aluminum hydroxide was also detected. The black color of the scale was likely due to black CuO. The high voltage in the Group I tests could be explained by the presence of nickel oxides, which decreased the electrical conductivity of the anode.

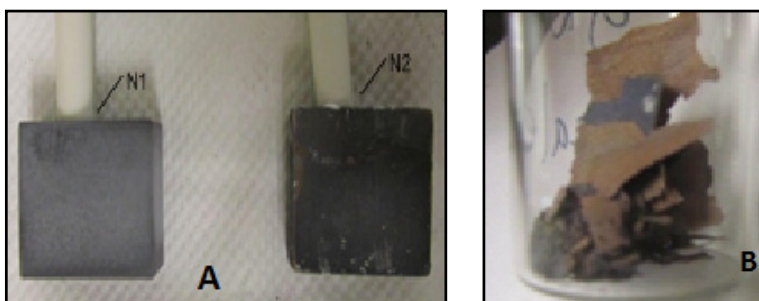


Figure 38 (A) Aluminum bronze samples covered with black scale after exposure above the electrolyte (Sample N1 was at 750°C for 2 hours, and Sample N2 was at 900°C for 1 hour.) (B) Detached scale from Sample N2

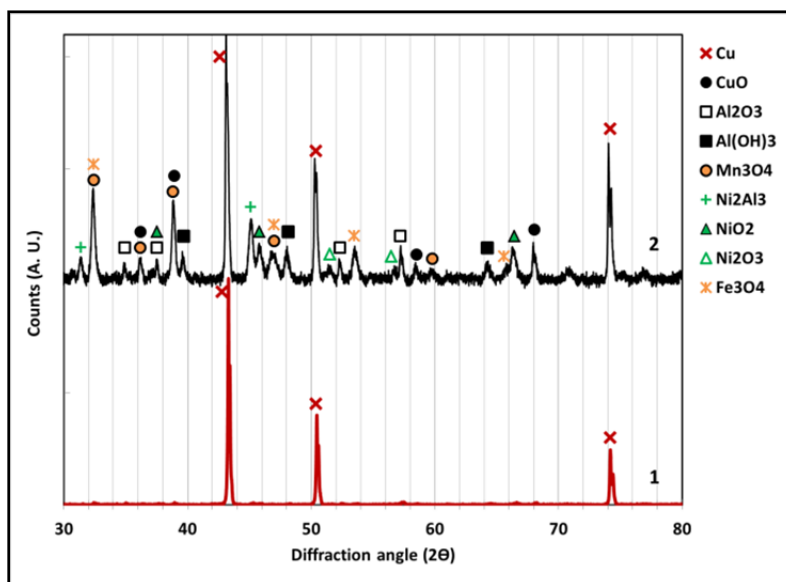


Figure 39 XRD spectra of the scale (Line 1 refers to the brown side facing the aluminum bronze, and Line 2 refers to the black side facing the electrolyte)

It was not surprising that the anode was covered with oxygen-containing scale. In fact, it was impossible to avoid moisture collecting on the electrolyte during its preparation. Moreover, as shown by LECO oxygen analysis, KF always contained about 0.3 wt% of oxygen, which could be ascribed to H₂O. Moisture vapors and high temperatures created conditions for the formation of oxides in the highest oxidation state on the anode surface prior to electrolysis.

It was assumed that pre-oxidizing treatment was not necessary for aluminum bronze anodes prior to electrolysis. It was found that it is beneficial to prevent the anode surface from contact with vapors while electrodes are suspended over the melt.

3.2.5 Purity of the Produced Aluminum Metal

To determine the quality of the aluminum metal produced, samples of it were withdrawn during electrolysis. An aluminum metal heel was added to the cell before electrolysis to allow aluminum samples to be taken during the early stages of electrolysis. Such tests are indicated by “EAL” in Table 5. The ICP analysis of the aluminum samples showed the concentration of impurities in the overall aluminum, which included the aluminum heel and the “instantaneous aluminum” (aluminum produced at the time of each sampling). The instantaneous aluminum was calculated according to the CE_{Ox} . Masses of the initial aluminum heel, withdrawn aluminum sample, and instantaneous aluminum were considered in calculating the content of impurities in the instantaneous aluminum. An example of calculated data for the mass overall aluminum and instantaneous aluminum and copper concentration in the aluminum for Experiment EAL11 is given in Table 6.

Metal impurities such as potassium, chromium, manganese, and nickel were not found in aluminum (the concentration, determined by ICP-EOS, was less than 0.05 wt%). However, copper, iron, and silicon were found. Figure 40 demonstrates the change in the copper, iron, and silicon content in overall aluminum during electrolysis in the KF-AlF₃ electrolyte at 700°C

Table 6 Copper content in the overall and instantaneous aluminum (Experiment EAL11)

Sample No.	Time of Sampling (h)	Mass of Produced Instantaneous Aluminum According to CE_{Ox} (g)	Mass of Overall Aluminum, Heel and Instantaneous (g)	Mass of Aluminum Withdrawn Sample (g)	Copper in Overall Aluminum, ICP Data (wt%)	Copper in Instantaneous Aluminum (wt%)
EAL11-1	0		400.57	0.1	0.06	0.00
EAL11-2	1	2.72	400.69	2.44	0.08	1.95
EAL11-3	4	16.40	419.78	3	0.07	0.18
EAL11-4	18	71.01	481.18	0.5	0.19	0.76
EAL11-5	21.5	80.53	494.62	5.86	0.21	0.78
EAL11-6	26.5	101.46	512.40	1.9	0.23	0.75
EAL11-7	29.0	110.09	520.03	3	0.24	0.76
EAL11-8	41.5	143.84	557.08	1.35	0.32	0.88
EAL11-9	44.5	149.94	563.03	0.77	0.33	0.89
EAL11-10	48.0	160.59	573.90 ^a		0.32	0.83

^a The weighed mass of overall aluminum after electrolysis was 560 g (the aluminum left on the cathodes was not considered).

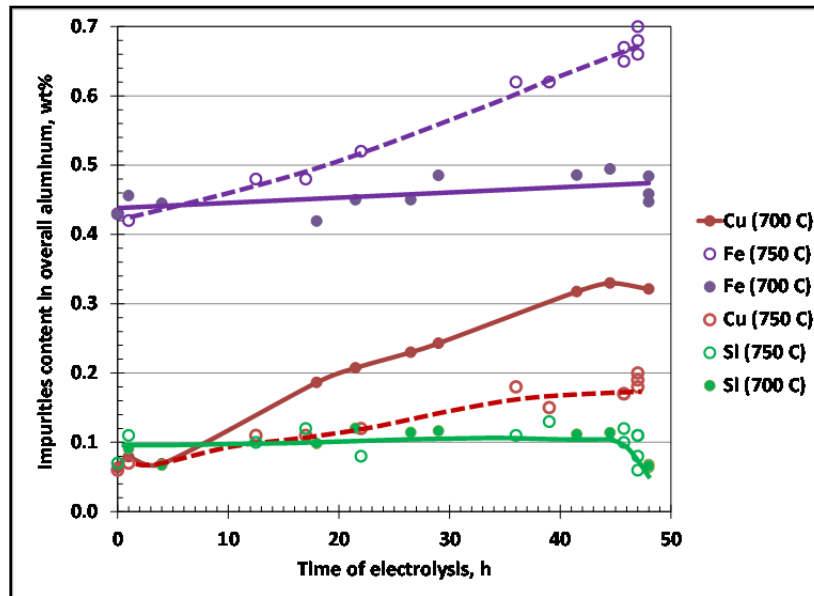


Figure 40 Content of copper, iron, and silicon in overall aluminum during electrolysis at 700°C (Experiment EAL 11) and 750°C (Experiment EAL 12)

(EAL11) and 750°C (EAL12). These tests differed only with regard to their operating temperature; all other experimental parameters were similar. Prior to electrolysis, the aluminum metal (heel) already contained 0.07 wt% copper, 0.4 wt% iron, and 0.1 wt% silicon. In both tests, the final concentrations of these metals were determined in three samples. One sample was withdrawn from the cell at the end of electrolysis, and two samples were drilled

out of the solid aluminum cake at the conclusion of each experiment. All data were close or equal to each other.

The silicon content in the aluminum did not depend on the temperature and was about 0.1 wt% in all samples throughout both tests (Figure 40). Only the last points on each curve indicate that the silicon content decreased sharply around the 48th hour. This change in the silicon content in the overall aluminum is difficult to explain. It is also not clear which form of silicon was present, Si or SiO₂, considering that silicon is probably not reduced on the cathode under conditions associated with low-temperature electrolysis in the potassium cryolite. This conclusion was based on the fact that the silicon concentration in the electrolyte did not change during 100-A, 100-hour electrolysis (Experiments 100E37 and 100E41; see Figure 7). Little attention was paid to the “silicon issue” in this work. The silicon contents in the electrolyte and aluminum were not measured in the same experiment, which would have enabled a direct comparison to be made.

Iron likely entered the electrolysis bath from the stainless steel cathode leads and from all parts of the cell made of stainless steel, such as the nuts and rods supporting alumina screens in the upper part of the cell. As shown in Figure 40, the Fe concentration in aluminum did not change significantly during electrolysis at 700°C, and it increased at 750°C. This did not contradict the general rule that the higher the temperature is, the higher the solubility of the metals in the molten salts is. Nevertheless, the copper content in the overall aluminum slightly increased during electrolysis at 750°C and increased more significantly at 700°C. This can be explained by the corrosion of the aluminum bronze anode during electrolysis at 700°C, which was a result of the aluminum droplets getting imbedded on the anode surface (Figure 41). In fact, the phenomenon of the aluminum droplets getting imbedded on the anode is attributed more to the electrolysis at 700°C than at 750°C, perhaps because of the lower viscosity of the molten aluminum at 700°C. The aluminum bronze anodes after 48 hours of electrolysis at 700°C (EAL11) and 750°C (EAL12) are shown in Figure 41.

In spite of the apparent increase in the copper content in the overall aluminum, its concentration in the instantaneous aluminum reached a constant value and did not change over time (Figure 42). Later, the same variation in the copper concentration in aluminum was confirmed in 100-A tests. In 100-A tests, the aluminum heel was never added to the cell; however, by 20–24 hours of electrolysis, enough aluminum metal was produced that sampling continued without any difficulties.

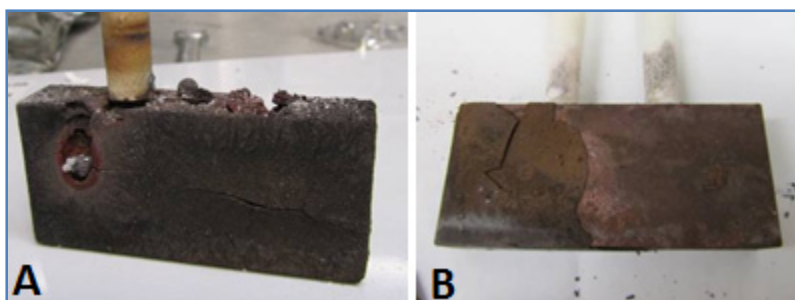


Figure 41 Aluminum bronze anodes after 48 hours of electrolysis in KF-AlF₃: A at 700°C (Experiment EAL11), B at 750°C (Experiment EAL12)

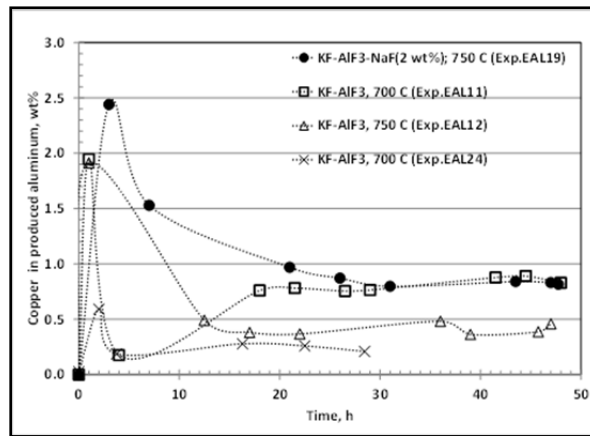


Figure 42 Copper content in the instantaneous aluminum metal produced during 20-A tests of Groups II and III (see Table 5)

The electrolyte samples taken during electrolysis were analyzed for the presence of impurities that could be caused by corrosion of the anode. Results indicated that the amount of copper, iron, nickel, and manganese in the electrolyte was less than the detectable limit of ICP-EOS (0.05 wt%) at any time during electrolysis. Consequently, the anode stability could be estimated with a high degree of reliability based on the amount of impurities in produced aluminum metal.

Figure 42 shows that the aluminum produced at the beginning of electrolysis in Group II and III tests (Table 5) contained the most copper impurity. After some time, however, the steady-state concentration of the copper impurity became constant. The level of copper in aluminum was in the range of 0.3–0.8 wt%. The aluminum was contaminated with the highest copper concentration at the beginning of the experiment, because only a small amount of aluminum had been produced. Furthermore, the electrodes submerged in the electrolyte were kept unenergized for some time before the electrolysis was started, which allowed the anode scale containing CuO (since CuO dissolves easier in cryolite than do Cu₂O and copper) to dissolve or even spall out (in cases of Group I tests).

If the anode surface was not in contact with the electrolyte vapors before being immersed in the electrolyte, the aluminum produced in the early stages of electrolysis did not contain impurities (Figure 43). Nevertheless, the concentration of copper in the aluminum did slowly increase and eventually reached a constant level of about 0.4 wt%. The higher the applied current density was, the faster a constant concentration of copper in aluminum was established.

The protective properties of the anode scale are determined by its formation (oxidation) process and dissolution process (corrosion). The presence of copper in produced aluminum is a result of the anode scale dissolution. It seems that the balance between the rate of the anode scale dissolution and the rate of aluminum production is maintained at a constant level during at least 50 hours of testing. In 20-A laboratory-scale electrolysis with a current efficiency of

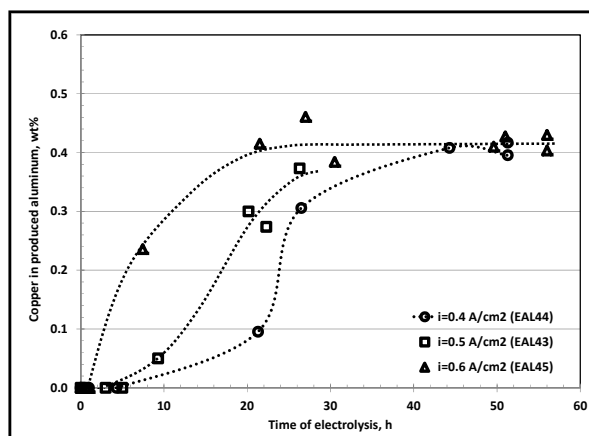


Figure 43 Copper content in the instantaneous aluminum metal produced in KF-AlF_3 electrolyte at 750°C at different current densities (Group IV tests, see Table 5)

about 60–80%, the concentration of copper in aluminum was found to be near 0.4 wt%. The amount of copper in aluminum was indicated by the current efficiency of the electrolysis, as seen in Table 3. The higher the current efficiency of a process is, the better the quality of the produced aluminum is.

3.3 100-A ELECTROLYSIS TESTING

3.3.1 Oxygen Content in Outlet Gas

The oxygen sensor did not detect the outlet gas oxygen concentration in all of the 100-A electrolysis tests. Several different strategies were tested to obtain an oxygen reading. These included increasing the cell temperature to 810°C , interrupting the current, changing the gas-carrier flow rate, and varying the position of the anode. None of these strategies were effective.

The last attempt to identify the oxygen concentration was undertaken in Experiment 100E41. A new oxygen sensor was used. Data are shown in Figure 44. Oxygen was successfully recorded during the first hour, but it slowly decreased from 22% to 0%. After the oxygen sensor completed an automated cleaning cycle, it worked for a short amount of time, detecting O_2 at about 20%, and then it quickly decreased to 0% again. If 20% O_2 is assumed for the entire experiment, the CE of this test would be 48% (at a gas flow rate of 1 L/min). The mass of oxygen in the outlet gas was calculated as follows:

$$m = V \times (d_{\text{mix}}) \times r, \quad [\text{L/L} \times \text{g/L} \times \text{L/min} = \text{g/min}]$$

where m is the mass (g/min) of oxygen in outlet gas passing through the oxygen sensor, V is the volume percent of oxygen in the outgas; d_{mix} is the density of the nitrogen and oxygen gas mixture at room temperature ($d_{\text{mix}} = d_{\text{N}_2} \times V_{\text{N}_2} + d_{\text{O}_2} \times V_{\text{O}_2}$), and r is the flow rate.

To confirm the oxygen sensor reading, gas chromatography (GC) was used to determine the O_2 content in a sample of outlet gas. The gas sample was taken during 1 minute with a 1-L syringe. The GC analysis determined that the oxygen concentration in the gas sample was about 16%. If

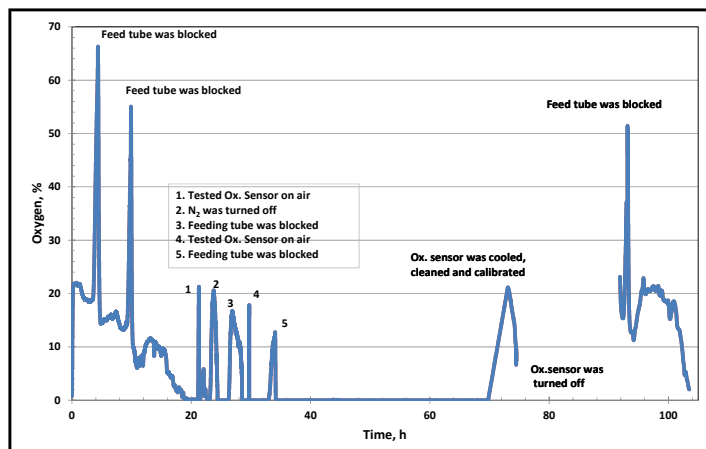


Figure 44 Oxygen sensor reading during 100-A electrolysis (Experiment 100E41)

16% O₂ was assumed for the entire experiment, the CE would be 46%. The oxygen mass was calculated as follows:

$$m = (M \times V)/22.4, \quad [(g/mol \times L/min)/L/mol = g/min]$$

Thus, in Experiment 100E41, the calculations of CE based on aluminum produced (50%), the oxygen sensor data, and the GC results were very close (Table A2). It is clear that the failed oxygen measurements were due to the oxygen sensor; however, the cause was not revealed.

3.3.2 Operating Parameters of the 100-A Electrolysis

All 100-A tests performed are listed in Table A2. A plot of a 100-A electrolysis test performed for more than 100 hours at 750°C is presented in Figure 45. The alumina concentration was about 5.5 wt%, which corresponds to the solubility of Al₂O₃ solubility in potassium cryolite with a CR of 1.3 at 750°C. The CR did not noticeably change during the experiment. The voltage and anode potential fluctuations were very similar. This means that the anode process determined the voltage. The cathode potential was very consistent, but around the 90th hour, there was a drop in voltage that can be explained as resulting from the anode touching the pool of aluminum at the bottom of the crucible. After the electrolysis was completed, the electrodes were left to cool in the melt, and the cell was cooled and then broken. The cathode in contact with aluminum is shown in Figure 46. The anode layer separated from the anode during cooling, as shown in Figure 47. For comparison, the view of the anode after 25 hours of testing (Experiment 100E27) is shown in Figure 48. The anode surface was not damaged. The anode scale spalled as the electrodes were raised out of the electrolyte and cooled.

An enhancement of the voltage and temperature from the same experiment (100E41) is shown in Figure 49. The crosses on the temperature curve correspond to the time of manual decreases in temperature. The temperature and voltage curves are inversely proportional; the temperature decrease led to an immediate voltage increase and vice versa. Consequently, the voltage fluctuation was followed by a temperature fluctuation. Still, at the end of the test, there were two abnormal voltage humps, while the temperature was almost constant. It was believed that such a large voltage fluctuation near the end of the test could be explained by aluminum metal getting imbedded on the anode surface, as shown in Figure 50. This occurred

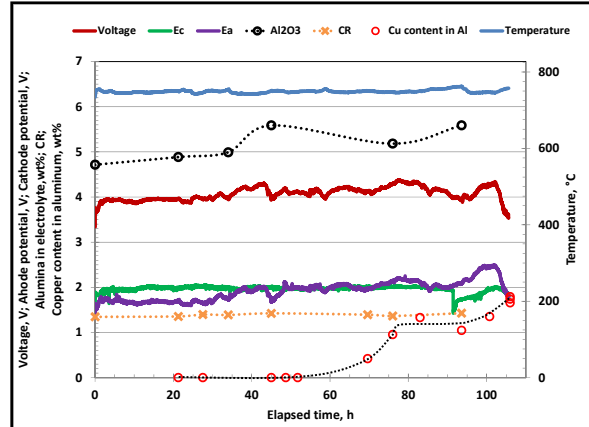


Figure 45 Operating parameters of 100-A electrolysis in KF-AlF₃ electrolyte (Experiment 100E41)



Figure 46 Electrodes, aluminum metal, and electrolyte cooled in the alumina crucible after 110 hours of 100-A electrolysis (Experiment 100E41), showing cathode in contact with aluminum



Figure 47 Anode scale separated from the anode during cooling (Experiment 100E41)



Figure 48 Aluminum bronze anode after 25 hours of 100-A electrolysis (Experiment 100E27), showing that the anode scale spalled out during cooling

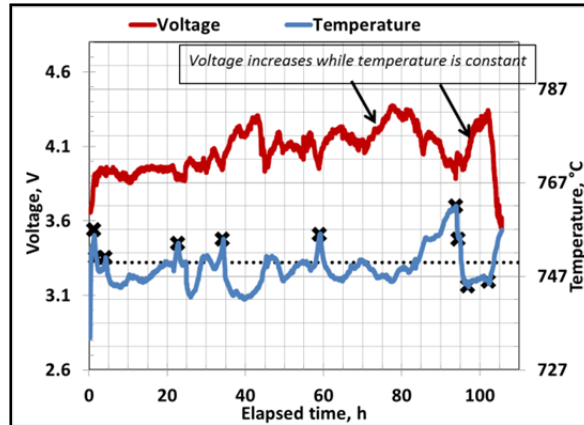


Figure 49 Asymmetrical change of voltage and temperature during a 100-A test (Experiment 100E41) (Crosses indicate the time when the temperature was manually adjusted. Dotted line is desired temperature of 750°C.)



Figure 50 Aluminum bronze anode after 100-A test (Experiment 100E41), showing aluminum metal droplets on the anode surface

because a large amount of aluminum had already been produced, and there was not enough space remaining in the cell, as seen in Figure 46. The aluminum samples were analyzed for copper (an aluminum heel was not added to the cell prior to the test). During primary stable electrolysis, the aluminum product was not contaminated. The copper concentration increased when the first abnormal voltage increase was observed. The copper content stabilized and increased again after the second voltage jump.

Data from another 100-A test (Experiment 100E37) performed for 80 hours are presented in Figures 51 and 52. The voltage was stable, and its fluctuation throughout the test was followed only by a change in temperature. The copper content in the aluminum was less than that found in Experiment 100E41; in the final product, it was 0.1–0.2 wt%. The anode and cathode potential curves (Figure 51) appear to be unusual after the 40th hour of electrolysis, but this is not reflected in the cell voltage and consequently was not a problem for the electrolysis

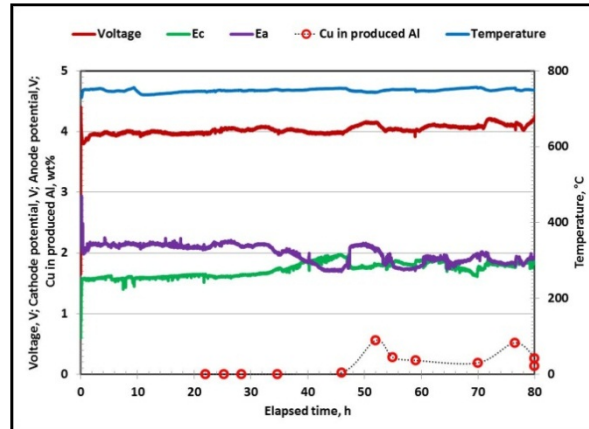


Figure 51 Operating parameters of 100-A electrolysis in KF-AlF₃ electrolyte (Experiment 100E37)

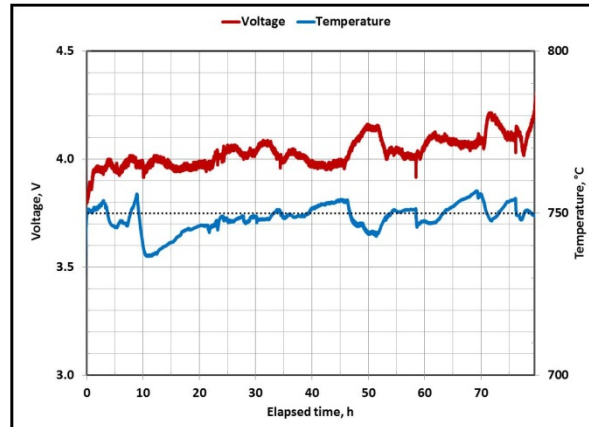


Figure 52 Asymmetrical change in voltage and temperature (Experiment 100E37)

process. The reason for this abnormal behavior during this test is not obvious, but it is thought that it could be attributed to the reference electrodes.

The instability of the voltage and the increased copper content in the aluminum product by the end of the 100th hour in the 100-A test was thus due to the aluminum metal droplets getting imbedded on the anode surface. The aluminum droplets dissolved the protective oxide layer, which resulted in copper contaminating the aluminum. However, the damaged spot on the anode surface can be recovered by the formation of a new oxide layer, which is reflected by the stabilization of the voltage and copper content in the aluminum. There is no doubt that the aluminum bronze anode performed very well in low-temperature electrolysis in potassium cryolite. Nevertheless, electrolysis in a laboratory-scale cell is definitely viable, depending on the electrolysis conditions and cell design.

3.3.3 Thickness of the Anode Scale

Figure 53 shows the thickness of the anode scale formed during 20-A and 100-A electrolysis tests versus the electrolysis time. Data from the two electrolysis tests are in good agreement. All results presented in Figure 53 are from tests performed in cells fitted with vertical electrodes: one aluminum bronze anode and two wetted cathodes at an anode current density of 0.45 A/cm^2 and an ACD of 2 cm. The thickness of the anode scale increased during about the first 50 hours of electrolysis, and then it stabilized at around 0.6–0.7 mm. The average thickness of the anode scales formed during 25 hours of 1,000-A electrolysis (i_c of 0.5 A/cm^2 and ACD of 2.2 cm) was 0.48 mm. Still, when the configuration of a cell or when the current density was changed, the thickness of the anode layer was different. For example, when the ACD was increased to 7 cm (Experiment 100E35) at the same anode current density (0.45 A/cm^2), the thickness of the anode scale reached 0.77 mm by the 28th hour of electrolysis. Different cell configurations were tested in Experiments EAL33 and EAL40. The thickness of the anode scale that formed during electrolysis in these tests differed from the basic line (Figure 53). In Experiment EAL40, an aluminum pool on the bottom of a crucible was used as a cathode. The cathode current density was about 0.25 A/cm^2 . The cathode in Experiment EAL33 was suspended by four rods, and the cathode current density reached 1.0 A/cm^2 . In both tests, an aluminum bronze plate of standard size was used as an anode.

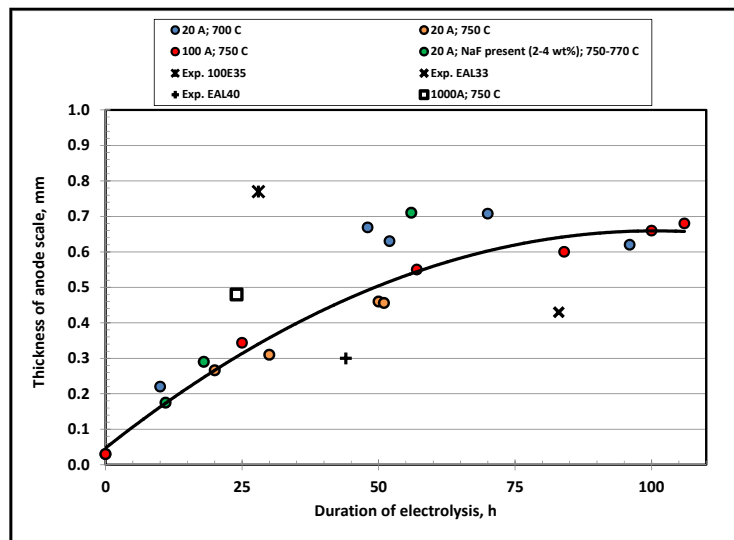


Figure 53 Thickness of the anode scale formed during 20-A, 100-A, and 1,000-A tests

No correlation was found between the anode scale thickness and the electrolyte composition (NaF presence) or between the anode scale thickness and the operating temperature (in a range of 700–770°C).

The anode scale that had detached from the anode surface after electrolysis in the KF-AlF_3 electrolyte at 750°C (Experiment 1000E) was analyzed by XRD. The scale from the side that faced the electrolyte contained Cu_2O (with traces of CuO) and K_3AlF_6 . The composition of the side that faced the aluminum bronze was Cu , Cu_2O , and KAlF_4 , which designated the electrolyte

penetration through the anode scale. XRD spectra are shown in Figure 54. A SEM-EDS elemental analysis of a rust anode flake determined that the dominant elements were fluorine, oxygen, potassium, aluminum, and copper. Traces of nickel, iron, and manganese were also present. To protect the anode scale from electrolyte penetration, further studies of the anode scale properties (density, porosity, etc.) should be done.

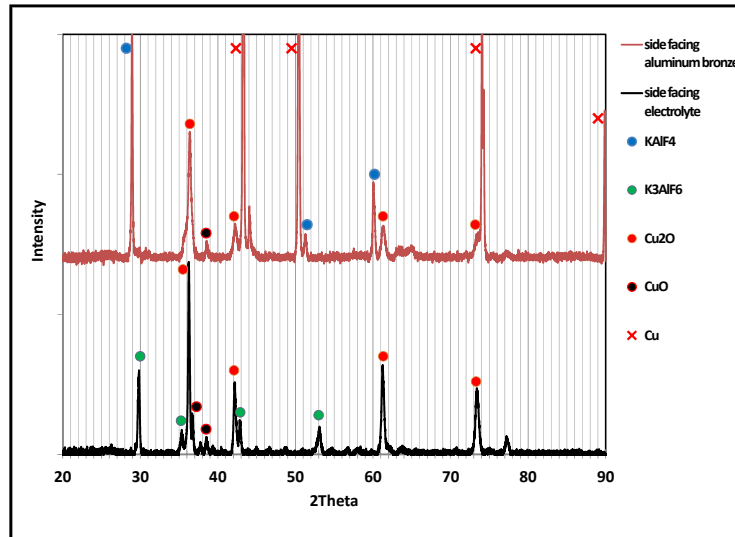


Figure 54 XRD spectra of anode scale obtained on the internal side (facing the aluminum bronze anode) and external side (facing the electrolyte) sides (Experiment 1000E)

The thickness of the anode scale is the result of two processes: its formation and its dissolution. Based on the data on the thickness of the anode scale, it was concluded that the growth of the oxide layer ended by approximately the 50th hour of electrolysis. After that, the balance between the rate of formation and the rate of dissolution was established. This equilibrium depends on numerous factors, including the current density, position and shape of the electrodes, and temperature. (The temperature impact was not noticeable in the tests that were performed because the temperature variation was insignificant.) The challenge is to sustain the formation-dissolution balance. In practice, however, the electrolysis process is complicated by unforeseeable conditions that could ruin the integrity of this protective layer.

3.4 MATERIAL TESTING

To determine the design criteria for the 1,800-A electrolysis cell, the following materials were tested for their corrosion resistivity to fluoride melts: nitride-bonded silicon carbide, tar-bonded silicon carbide, and boron nitride AX05.

3.4.1 Material Sample Testing

Samples of nitride bonded silicon carbide (SiC) and boron nitride (BN) AX05 were tested in an inert nitrogen and air atmosphere. Samples were half immersed in the KF-AlF₃ (CR of 1.3)

electrolyte saturated with alumina at 750°C. The sample weight and size were measured periodically. The test conditions and results are presented in Table 7.

Table 7 Conditions and results of material tests in the KF-AlF₃ Al₂O₃-saturated electrolyte with a CR of 1.3 at 750°C

Sample Material	Conditions	Exposure Time	Results
SiC (nitride-bonded)	Nitrogen flow; graphite crucible	380 h	The weight increased by 10% (from 1,130.7 to 1,233.0 g) during the first observation during 103 hours of exposure in the melt, but its size did not change. Although the weight and size did not change during the next 273 hours, the sample and walls of the crucible, especially in the interface area, were covered with a thin, fragile, metal-like layer.
BN (AX05)			The weight and size did not noticeably change during the test.
BN (AX05)	Air; aluminum metal was placed on the bottom of the alumina crucible	506 h, removed, measured, put back for 950 h	A slight increase in the weight and thickness was observed; it was likely due to buildup of the solid electrolyte on the sample surface, especially near the interface.

A BN AX05 sample that had been exposed for 950 hours to air and a KF-AlF₃ electrolyte that was saturated with alumina and that contained molten aluminum metal on the bottom of the crucible was removed and observed periodically. The bottom half of the sample was immersed in the electrolyte and molten aluminum, and the top half remained in the air. The weight and thickness at specified positions of the sample were recorded. The solid electrolyte built up at the interface of the air and electrolyte (Figure 55). The portion of the sample that was immersed in the electrolyte changed from white to gray. No significant deterioration was

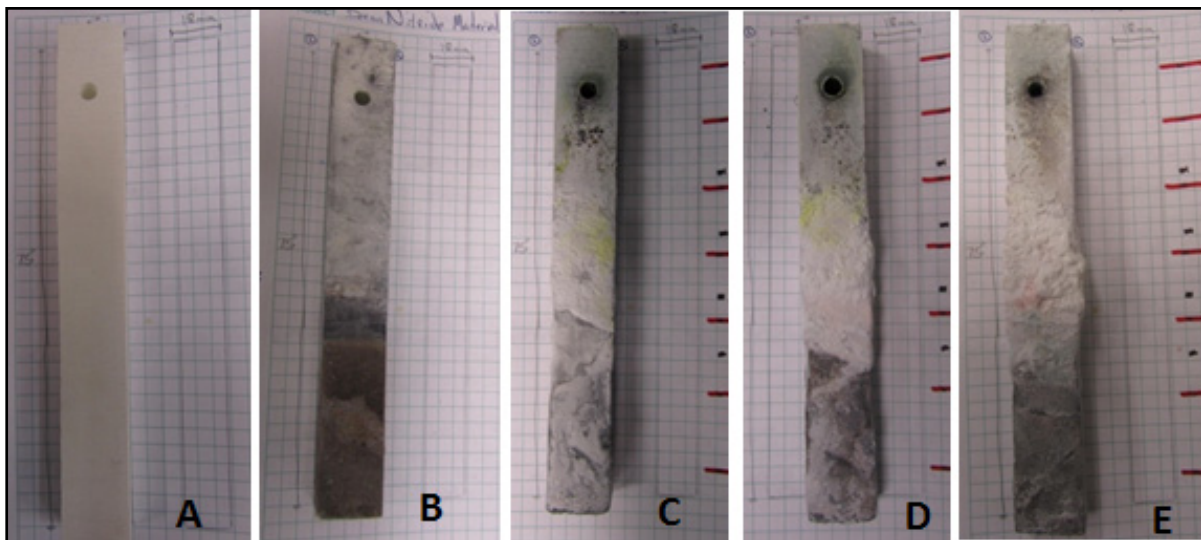


Figure 55 Views of BN sample exposed to KF-AlF₃ electrolyte and molten aluminum at 750°C after 0 (A), 178 (B), 410 (C), 575 (D), and 950 (E) hours

observed on the surface of the sample, even after 950 hours. The weight of the sample increased 5% because it was difficult to remove all of the solid electrolyte crust. The difficulty in removing the crust (near the interface) caused the thickness of the sample to vary. The portion of the sample that was immersed in the electrolyte and molten aluminum got only 1 mm thicker (Figure 56).

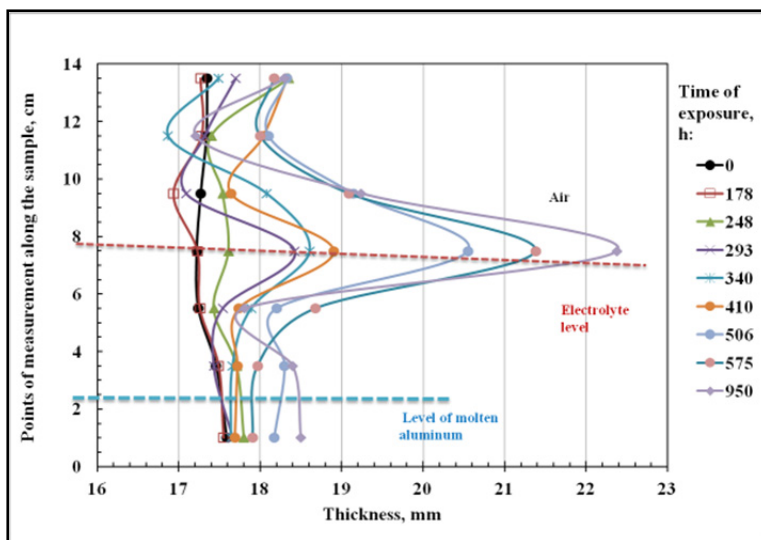


Figure 56 Thickness of the BN sample exposed to the KF-AlF_3 electrolyte and molten aluminum at 750°C for 950 hours

It was concluded that BN AX05 can withstand being exposed to potassium cryolite electrolytes during aluminum electrolysis and be used as a construction material.

3.4.2 Material Testing at Electrolysis Conditions

An electrolysis test using a tar-bonded SiC crucible at a current of 25–50 A and temperature of $710\text{--}740^\circ\text{C}$ was performed for 47 hours. Observation of the crucible revealed no damage, but the its bottom became very flaky. A sparkling black substance covered the alumina cases, wall crucible area above the melt, and aluminum cake on the bottom. The aluminum metal obtained was contaminated with a large amount of silicon.

Since the BN AX05 material had very good resistivity to the molten potassium cryolite, it was used to construct a 10-A electrolysis cell for a prototype of the 1,800-A cell. The BN crucible was built by using five pieces of BN glued together with 903-alumina adhesive. Thermeez alumina putty, 903-alumina adhesive, and BN spray were all tested as glues to hold together the BN pieces. The 903-alumina adhesive exhibited the best results. A BN crucible was inserted into a stainless steel shell. Thermeez Alumina putty, 903-alumina adhesive, and BN spray were tested as a cover material for preventing the external walls of the shell from oxidizing. The BN cover provided the stainless steel shell with the most protection. It could withstand the heating and cooling of the experiment, and no corrosion was observed. A view of the BN crucible with molten electrolyte inside the stainless steel shell is given in Figure 57.

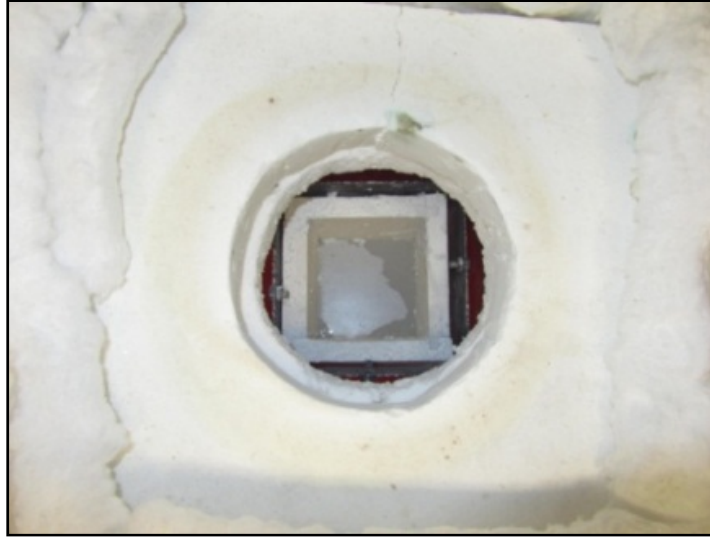


Figure 57 View from above of a BN crucible with molten electrolyte inside a stainless steel shell placed in a furnace

A 10-A electrolysis test (Experiment E-42) with one aluminum bronze anode and one wetted cathode was performed in the crucible that was constructed. The anode current density was 0.5 A/cm^2 , and the cathode current density was 0.65 A/cm^2 . The electrolysis lasted for 42 hours. The voltage and the anode and cathode potentials were stable throughout electrolysis.

To determine if the BN crucible in the stainless steel shell could be reused, the crucible with the molten electrolyte was kept for 24 hours at 740°C . The electrolyte was poured out of the crucible and set to cool three times. No signs of cracking were observed.

3.5 1,000-A ELECTROLYSIS TEST

Aluminum electrolysis was performed at a current of 1,000 A, at a temperature of 750°C , and in a cell fitted with vertically oriented aluminum bronze anodes and wetted cathodes. The cell included a total of six anodes and cathodes with a current density of 0.5 A/cm^2 and an ACD of 2.2 cm.

An electrolysis bath was fabricated from a stainless steel container, in the shape of a rectangle. A BN crucible was placed inside this container (Figure 58). The whole bath was covered with a stainless steel cap that gave access to the electrolysis leads, thermocouple, feeding tube, and outlet and inlet gas. This cap was insulated with fiber-ceramic on the side that was exposed to the electrolyte. The bus bar was constructed in a way that the distance between the anodes and cathodes could be adjusted. The bus bar for the anodes was made of aluminum bronze, while the bus bar for the cathodes was made of stainless steel (Figure 59). Alumina was delivered to the cell through two feeding tubes positioned in two different locations on the cap. The flow of nitrogen gas was kept at 10 L/m.

A scrubber purification system was specially developed for the 1,000-A tests (Figure 60). It was composed of three columns, the first of which was filled with glass wool to collect solid particles in the outlet gas. The second column was filled with dried alumina to absorb residual

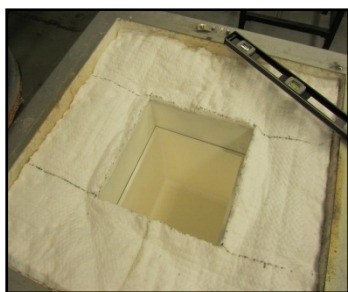


Figure 58 BN crucible inside of the stainless steel shell placed in the furnace



Figure 59 Bus bars for anodes and cathodes



Figure 60 Scrubber purification system

hydrogen fluoride (HF) and traces of moisture. The final column was empty to prevent the possibility of alumina contaminating the oxygen sensor. The outlet gas, whose rate was slightly higher than the input gas rate, was drawn from the cell by using a pump and controlled by a valve. This created a slightly negative pressure within the chamber.

After the pre-prepared electrolyte (71 kg) was added to the bath, the shroud was mounted on the furnace used to support the cap with the electrode and bus bar system (Figure 61). The furnace was heated in a nitrogen atmosphere at a rate of 50°C/h. When the temperature of the furnace reached 750°C, the shroud was removed and the electrodes were lowered into the electrolyte. The unenergized electrodes were in the molten electrolyte for 30 minutes. This amount of time was needed for the electrodes to reach 750°C and for the electrodes to be connected to the power supply. The setup with the electrolysis in progress is illustrated in Figure 62.



Figure 61 View of furnace when electrolysis is in progress



Figure 62 Shroud mounted on furnace supporting system of electrodes and bus bars

Plots of the 1,000-A electrolysis are provided in Figures 63 and 64. At the beginning of the electrolysis, the current was increased in steps (250, 500, 750, and 1,000 A), with each step taking approximately 15 minutes. The voltage stabilized near 4 V. An oscillation of about 150 mV was indicated. The electrolysis was sustained, and no voltage fluctuation was observed.

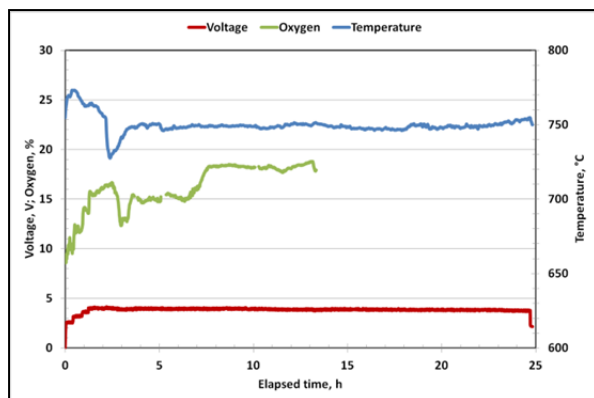


Figure 63 Plot of the 1,000-A electrolysis

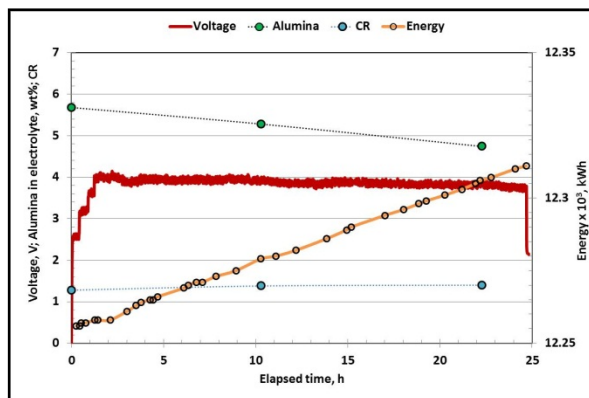


Figure 64 Changes in voltage, alumina content in the electrolyte, CR, and energy expended on maintaining the furnace's heat during 1,000-A electrolysis

The temperature setpoint was difficult to determine due to the slow response time of the furnace. During the first 3 hours, the temperature was manually adjusted to the desired 750°C. After the temperature was set, no changes in temperature were observed.

Oxygen in the outlet gas was detected by an oxygen sensor. With any change in current, there was an instant change in oxygen, which proved the consistency of the electrolysis. After the third hour, there was a sharp decrease in oxygen, followed by a decrease in temperature. Between 7 and 8 hours of electrolysis, there was a noticeable increase in oxygen that was difficult to explain at that moment. The oxygen stabilized at this new level, however. Such constancy in the amount of oxygen in the outlet gas further confirmed the stable course of the electrolysis.

Samples of electrolyte were withdrawn during electrolysis and analyzed for oxygen, potassium, aluminum, and copper. At the beginning of electrolysis, the alumina concentration in the electrolyte was close to its solubility limit, but it slowly decreased during electrolysis because of feeding interruptions (Figure 64). The CR remained constant throughout the entire test. Copper was not found in the electrolyte. The energy expended on maintaining the furnace heat during the 1,000-A electrolysis was recorded to be 2.2 kWh/h.

After electrolysis, the anodes were covered with a dense oxide layer. Pictures of the electrodes suspended over the melt just after electrolysis was stopped and of them about to be mounted on a shroud for cooling are shown in Figures 65 and 66. During cooling, the anode scale cracked and fell away. The scale on the anode surfaces that faced a cathode had nearly identical thicknesses (0.49 mm on average). However, the scale on the anode surfaces that faced away from the cathode were thinner (0.35 mm). All of the anodes looked identical, no matter what their position was in the cell (inside or outside). Changes in the anode dimensions due to corrosion were not observed, and aluminum droplets previously found imbedded on the anode surface of other samples were not present. Cathodes between anodes had a smooth surface. The outside surface of one cathode and the top edges of the cathodes (that faced the bus bar) had some solid crust. All alumina shields that covered current leads had dissolved in the

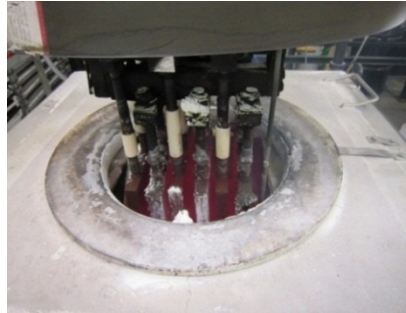


Figure 65 After electrolysis, electrodes suspended above melt



Figure 66 Cooling electrodes about to be mounted on shroud

electrolyte due to inadequate feeding. The stainless steel bus bar was significantly corroded, while the aluminum bronze bus bar was covered with a black protective layer.

After electrolysis was completed, the electrolyte was ladled out of the cell. Only a portion of the aluminum metal produced could be taken out of the cell because of the size of the ladle. As a result, the CE could not be measured by using the mass of aluminum produced. In order to estimate the CE of the 1,000-A electrolysis test, the resistivities of the cell contents (molten electrolyte and aluminum) were measured by using two molybdenum wires fixed inside an alumina tube. The data obtained are shown in Figure 67. The value of the resistivity changed one order of magnitude at a distance of 1.5 cm from the bottom. It was assumed that the aluminum metal pool on the bottom of the crucible was about 1.5-cm high, which represents about 5,656 g of aluminum (the density of molten aluminum is 2.357 g/cm³ at 750°C). Thus, the CE was about 70%. The low CE was a result of inadequate feeding. The CE could be increased by raising the cathode current density and temperature (by about 20°C).

The content of sodium in the electrolyte changed from 0.14 to 0.18 wt% by the end of the test. Copper was not found in the electrolyte samples, whereas it was present in the aluminum metal, at about 2.8 wt%. The elevated copper content in the aluminum produced was explained by the fact that the electrodes were immersed in the molten electrolyte without being energized for 30 minutes prior to electrolysis. This allowed the surface of the anodes to dissolve in the electrolyte. The initial copper contamination of the aluminum was not considerably reduced by the relatively small increase in the aluminum mass during 24 hours of electrolysis. Another reason why the aluminum metal contained significant amount of copper might have been the constantly decreasing alumina concentration in the electrolyte due to feeding interruptions. A decrease of O²⁻ ions in the melt leads to the shifting of the $\text{Cu}_2\text{O} \rightarrow 2\text{Cu}^+ + \text{O}^{2-}$ balance to the right and to the dissolution of the anode oxide scale. Note that no anode corrosion and no changes in the size of the anode was observed.

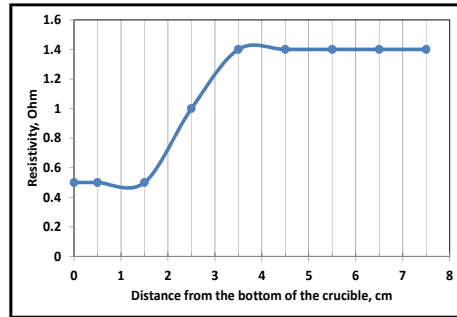


Figure 67 Resistivity of the electrolyte and molten aluminum vs. distance from the bottom of the crucible

Based on the 1,000-A electrolysis test data, the following conclusions were drawn:

1. The electrolysis of aluminum in a 1,000-A bath equipped with a system of inert anodes–wetted cathodes in the potassium cryolite electrolyte at 750°C was stable and sustained.
2. The construction of bus bars had sufficient electrical conductivity and did not notably increase the cell voltage. The stainless steel bus bars were significantly corroded; in the future, they will have to be insulated or replaced with another material.
3. A developed scrubber purification system worked very well. However, the outlet tube made of stainless steel was corroded, and outlet gas could not pass through.
4. The automatic feeding system needs to be improved, since alumina powder often jammed in the Teflon tubing. Moreover, the location of feeding tubes needs to be changed in such a way that the alumina will fall down between the crucible wall and electrodes (not over the electrodes).
5. In order to avoid solid crust on the cathodes, either the temperature should be slightly higher than 750°C or all the cathodes should be placed between anodes.

This page intentionally left blank

4 BENEFITS ASSESSMENT

The commercialization of this technology will have a significant impact on the primary aluminum industry and result in significant energy, environmental, and economic benefits for the United States. Energy benefits will arise from the reduced amount of energy consumed on site for aluminum production. The primary source used to estimate energy savings was *U.S. Energy Requirements for Aluminum Production*, prepared for the DOE-EERE ITP in February 2007 [47]. Specifically, Table M.2 in Appendix M (page 132) of that document was used as a reference for calculations.

Table 8 U.S. energy requirements for aluminum production

Aluminum Production Technology	Column A: Energy required for typical modern Hall-Héroult cell operating at 95% current efficiency and ACD of 4.5 cm		Column B: Energy required for inert anode operating at 95% current efficiency, with oxygen polarization differences and an ACD of 2 cm with wetted cathode		Column C: Energy required for new vertical multipolar technology at 95% CE with oxygen polarization difference, 2.0 cm ACD with wetted cathode, metal anode, lower current density, and lower-temperature operation	
	V (dc)	kWh/kg Al	V (dc)	kWh/kg Al	V (dc)	kWh/kg Al
Reaction itself	1.20	3.76	2.20	6.90	2.37	7.43
External	0.15	0.47	0.15	0.47	0.15	0.47
Anode	0.30	0.94	0.30	0.94	0.09	0.28
Anode polarization	0.55	1.73	0.10	0.31	0.10	0.31
Cathode polarization	0.05	0.16	0.05	0.16	0.05	0.16
Cryolite bath	1.75	5.49	0.78	2.44	0.41	1.29
Cathode	0.45	1.41	0.45	1.41	0.30	0.94
Other	0.15	0.47	0.15	0.47	0.06	0.19
Cell total	4.60	14.43	4.18	13.11	3.53	11.07
Energy savings				9%		24%
Anode manufacturing		0.61		0.77		0.01
Total on-site cell and anode		15.04		13.87		11.08
Energy savings				8%		26%

Column A outlines the energy requirements for a typical Hall-Heroult operation (2007), including the use of a standard bath (NaF-AlF₃) at 960°C, carbon anodes and cathodes, and a current density of 0.85A/cm². Column B (Column D in the referenced Table M.2) outlines the energy requirements with cermet inert anodes, wetted cathodes, and reduced ACD, while the same bath composition and operating temperature are maintained. Column C outlines the energy requirements for the technology under development in this report. The technology allows for further energy savings versus those achieved in the previous best-case scenario (Column B). These energy savings would result from the use of metal anodes, a lower current density, lower-temperature operation, and lower energy intensity of anode manufacturing. The specific assumptions are described in the following text.

The first point to note is that although the energy required for the reduction reaction is higher when oxygen-emitting inert anodes rather than carbon anodes are used, this voltage penalty is more than overcome by the savings in anode polarization (0.45 V) and in the reduced ACD (0.97 V) that result from the use of wetted cathodes. The theoretical reduction voltage is actually higher for the new technology because of the lower operating temperature (at 700°C, the decomposition voltage is 2.37 V versus 2.20 V at 960°C). However, since the decomposition reaction is endothermic, and the primary source of heat to maintain an isothermal reaction is electrical, the overall energy requirement for reduction would be similar, since the enthalpy for the reaction at 700°C is close to that at 960°C. For a detailed discussion of the energy requirement, see the 2007 *U.S. Energy Requirements for Aluminum Production* report [47].

The use of a metal anode with higher conductivity versus a potential cermet inert anode in Column B (which is assumed to have electrical conductivity similar to conventional carbon anodes) saves an additional 0.21 V.

The reduction in current density from 0.85 A/cm² in Columns A and B to 0.45 A/cm² in Column C leads to a further reduction of 0.37 V in cell voltage. Present-day operations typically increase the current density in order to increase cell productivity. Higher current densities result in higher specific energy costs but lower specific labor and capital costs. The technology being developed for this project can operate at various current densities. However, since all the technical and economic feasibility data for this technology that have been developed to date have been based on a current density of 0.45 A/cm², this value is used to determine energy benefits.

For the “cryolite bath” energy requirement, it is also assumed that the electrical conductivity of the bath is the same for both technologies. The actual electrical conductivity of the low-temperature potassium-based electrolyte is unknown, but it can be either higher or lower than that of the conventional electrolyte because of differences in both the composition and the operating temperature. The alumina concentration appears to be an important parameter. It is assumed that the electrical conductivity in both baths is similar.

Savings at the cathode are mostly related to heat loss for the cell. A conservative estimate is that the heat loss at 700°C is reduced by one-third; therefore, the voltage loss at the cathode is 0.30 V versus 0.45 V in pots (i.e., electrolysis cells) operating at 960°C. Heat loss savings that arise from the redesigned cell with vertically oriented electrodes have not been considered here, but they are expected to be significant as well.

For the “other” energy requirement component, an energy benefit of 0.09 V for a lower operating temperature is claimed for this technology. The savings comes from the lower enthalpy in the aluminum product at 700°C versus at 960°C in conventional electrolysis cells, since the heat value of the aluminum produced at 960°C in conventional cells is not recovered in present practice.

Finally, it is assumed that energy savings result from metal anode manufacturing (0.60 kWh per kg of aluminum). The new technology will use commercially available aluminum-bronze metal inert anodes. The energy required to manufacture the anodes from this alloy is minimal relative to the expected 6-year service life of these anodes, which produce 7.93 kg of aluminum in 6 years per cm³ of anode (assuming anodes that are 1-cm thick, a service life of 52,560 hours, and a current density of 0.45 A/cm²). Assuming the alloy requires slightly less energy than

aluminum (e.g., 10 kWh/kg of alloy), this would equal about 0.07 kWh/cm³ of alloy (assuming a density of 7 g/cm³). Since 1 cm³ of anode produces 7.93 kg of aluminum during its life, the contribution of the anode alloy to the energy requirement for aluminum is less than 0.01 kWh/kg of aluminum.

Therefore, the overall **on-site** energy savings of the proposed technology is 3.96 kWh/kg of aluminum, which represents a 26% savings versus the baseline reduction technology (15.04 kWh/kg) that includes anode manufacture. U.S. primary production capacity dropped from more than 4 million tonnes in the 1980s and 1990s to 2 million tonnes in 2011, primarily because older U.S. smelters became uncompetitive and were shut down. This lost capacity can be restored by implementing the new energy-efficient technology described in this proposal. It is estimated that this technology will produce 2.5 million tonnes of aluminum by 2030, given that prototype testing occurred in the 2015–2018 timeframe, with commercial demonstration of a full potline by 2022. Given that the U.S. grid average is 10,000 Btu/kWh, this technology would save 100 trillion Btu/yr in 2030.

The 2007 *U.S. Energy Requirements for Aluminum Production* report [47] prepared for the DOE-EERE ITP also summarizes the reduction of carbon dioxide equivalent (CO₂-eq) emissions for various aluminum production technologies. As indicated in Table E.4 (page 110) in the report, conventional Hall-Heroult aluminum production results in emissions of 10.62 kg CO₂-eq/kg of aluminum, while using the technology associated with the inert anodes and wetted cathodes results in emission of 6.29 kg CO₂-eq/kg of aluminum. The savings is 4.33 kg CO₂-eq/kg of aluminum. Assuming 2.5 million tonnes of aluminum are produced in the United States in 2030 by using this technology, the savings would amount to more than 10 million tonnes/yr of avoided greenhouse gas emissions. In addition, all perfluorocarbon (PFC) emissions arising from anode effects in current practices would be eliminated, since the inert anodes do not contain carbon.

Economic benefits associated with the new technology would also be significant. The cost component breakdown for aluminum production was estimated by Stuart Burns and published in the February 2009 issue of *Metal Miner* [48]. His analysis suggests the following cost structure for primary aluminum production, based on a breakeven price of \$1,300/tonne of aluminum:

- Alumina – 30%,
- Electricity – 24%,
- Anodes – 15%,
- Labor – 8%,
- Gas – 2%,
- Chemicals – 10%,
- Spares – 8%, and
- Overhead – 3%.

This analysis suggests that the economic advantage of the proposed technology results from the avoidance of anode manufacture (15%) and the reduced cost of on-site electricity (27% of 24%), for a total benefit of 21.5% of the breakeven aluminum production cost, or \$280 per

tonne of aluminum. This savings provides sufficient incentive to implement this transformational aluminum production technology once the concept is demonstrated in a prototype full-scale cell. In addition, this technology could re-vitalize the primary aluminum industry in the Pacific Northwest, which was shut down in the early 2000s due to high electrical costs and process inefficiencies related to the age of the smelters. This technology could utilize much of the infrastructure in the region.

5 COMMERCIALIZATION

The strategy for rapidly deploying the technology is to successfully demonstrate retrofitting an entire cell into an existing potline. Once this is achieved, the existing pots can be swapped out as they come out of service, or earlier if economics suggest. This process can proceed until the entire line is converted to the new technology. The same strategy (in which a suitably-sized prototype cell is integrated in an existing line) can be applied to other potlines. The older, inefficient lines should be targeted for early conversion. Since most of the modern new efficient smelters are being built off shore, the logical locations for implementing the technology (i.e., retrofitting) would be in the United States, especially in the Pacific Northwest where many of the older plants are mothballed. Because energy and environmental benefits reduce the breakeven price point of aluminum by \$280/tonne, it is likely that the technology would penetrate the commercial market rapidly.

This page intentionally left blank

6 ACCOMPLISHMENTS

The following publications and presentations resulted from this project:

1. Hryn, J., O. Tkacheva, and J. Spangenberg, 2013, "Initial 1,000A Aluminum Electrolysis Testing in Potassium Cryolite-Based Electrolyte," *Light Metals*, pp. 1289–1294; also presented at the 2013 TMS Annual Meeting, San Antonio, Texas, March 3–7, 2013.
2. Tkacheva, O., J. Hryn, J. Spangenberg, B. Davis, and T. Alcorn, 2012, "Operating Parameters of Aluminum Electrolysis in a KF-AlF₃ Based Electrolyte," *Light Metals*, pp. 675–680; also presented at the 2012 TMS Annual Meeting, Orlando, Fla., March 11–15, 2012.
3. Hryn, J.N., 2011, "Ultra-High Efficiency Aluminum Production Cell," EIP Portfolio Review Meeting, Golden, Colo., June 14–15.
4. Tkacheva, O., J. Spangenberg, B. Davis, and J. Hryn, 2011, "Aluminum Electrolysis in an Inert Anode Cell," Molten Salt Chemistry and Technology (MS9), Trondheim, Norway, June 5–9.
5. Tkacheva, O., J. Spangenberg, N. Carter, B. Davis, and J. Hryn, 2010, "Aspects of Low-Temperature Electrolysis of Aluminum in Metal Inert Anode Cells, Non-Ferrous Metals," Krasnoyarsk, Russia, Sept. 2–4.
6. Hryn, J.N., 2010, "Metal Alloy Anodes in Aluminum Electrolysis," Sadoway60 Symposium, Massachusetts Institute of Technology, Cambridge Mass., June 9–11.

This page intentionally left blank

7 CONCLUSIONS

Sustained operation of the aluminum electrolysis process in 20-A and 100-A cells fitted with vertical aluminum bronze anodes and wetted cathodes was achieved in a potassium-cryolite-based electrolyte in a temperature range of 700–770°C

The NaF accumulated during long-term electrolysis in an electrolytic bath affects the liquidus temperature of the molten mixture. To take the NaF content in the electrolyte into account, it is necessary to adjust the operating temperature. It is recommended that the minimal operating temperatures for electrolysis in KF-AlF₃-NaF (2 wt%) electrolytes and in KF-AlF₃-NaF (4 wt%) electrolytes be as high as 750°C and 770°C, respectively.

To avoid voltage instability caused by the formation of cathode incrustation, the temperature of the electrolysis cell should not be below 700°C. Moreover, it is recommended that the temperature for the electrolyte before the electrodes are lowered and electrolysis is begun be 770°C.

The voltage anomalies that occur during electrolysis with inert anodes are mainly produced by the anode processes. A decrease in voltage, after it has been stable, signifies anode corrosion, while a rise in voltage is related to anode passivation.

The presence of oxide scale on the surface of the aluminum bronze anode before electrolysis significantly affects the cell voltage values, current efficiency, and amount of impurities in the produced aluminum. It is recommended that any contact between the anode surface and the electrolyte vapors be prevented.

The constant level of copper in produced aluminum during electrolysis in 20-A cells indicates that a balance between the rate of anode scale dissolution and the rate of aluminum production has been established. This balance can be shifted by increasing the current efficiency of the process, which will result in produced aluminum with a lower level of contamination. It is recognized that even in 100-A tests, the purity level of the aluminum can vary due to circumstances associated with cell operations that would not occur in industrial-scale cells over longer times.

Design criteria for a semi-industrial electrolysis cell were developed based on the 20-A and 100-A testing. An initial 1,000-A test was successfully performed. Aluminum electrolysis occurred in a BN-lined cell containing a potassium cryolite bath (CR of 1.3) at 750°C, with three pairs of vertically aligned aluminum bronze anodes and wetted cathodes (ACD of 2.2 cm), and with automated alumina feeding. It demonstrated sustained aluminum production at 1,000 A (current density of 0.5 A/cm²) for 24 hours at 4 V without significant voltage fluctuations (<150 mV). Furthermore, the aluminum bronze anodes formed a dense, stable, protective, and electrically conductive scale (0.48 mm) composed of Cu₂O and CuO.

Finally, a limiting factor in implementing inert anode technology has been the cell container material coming in contact with the bath. In this project, BN (Saint Gobain Grade AX05) proved to be an effective and durable liner material for the cell.

This page intentionally left blank

8 RECOMMENDATIONS

Four areas need to be investigated further before scaling of the technology can be economically justified

1. Issues related to aluminum purity, which appear to be associated with anode scale formation, need to be understood. In previous tests, the copper levels in the aluminum product increased at times when the voltage fluctuated. An understanding of these fluctuations appears to be a key for achieving long-term aluminum production without contamination. Long term tests must be done to develop this understanding.
2. BN has been identified as a suitable container material, but cost issues remain a concern. The key requirements to be met in order for cell materials to be used economically at production scale need to be determined and understood.
3. The steady-state level of sodium in the cell needs to be determined through a better understanding of sodium losses (either through the vapor phase, in the aluminum product, or through an electrolyte bleed system). Sodium enters the cells as an impurity in the alumina feed.
4. Metal cathodes have worked well, but specific compositions need to be tailored to minimize the contamination of the aluminum product by cathode materials.

In addition, operational parameters need to be improved. Bus bars that had sufficient electrical conductivity and did not notably increase the cell voltage were constructed. The stainless steel bus bars were significantly corroded and will have to be insulated or replaced with another material, likely aluminum bronze.

The developed scrubber purification system worked very well. However, the outlet tube made of stainless steel corroded. Again, aluminum bronze material would likely improve scrubber performance.

Finally, the automatic feeding system needs to be improved, since alumina powder often plugged the Teflon tubing. Moreover the feeding tubes should be re-located in such a way that alumina would be fed to the cell between the crucible wall and electrodes and not over the electrodes.

This page intentionally left blank

9 REFERENCES

1. Pawlek R.P., 2008, "Inert anodes: An update." *Light Metals*, pp. 1039–1045.
2. Grjotheim K., Krohn C., Malinovsky M., Matiasovsky K., and Thonstad J., 1982, *Aluminium Electrolysis. Fundamentals of Hall-Heroult Process*, 2nd Edition, Dusseldorf: Aluminium-Verlag.
3. Skybakmoen E., Solhiem A., and Sterten A., 1997, "Alumina solubility in molten salt systems of interest for aluminum electrolysis and related phase diagram data," *Metallurgical and Materials Transactions*, 28B, p. 81.
4. Robert E., Olsen J.E., Danek V., Tixon E., Ostvold T., and Gilber B., 1997, "Structure and thermodynamics of alkali fluoride-aluminum fluoride-alumina melts. Vapor pressure, solubility, and Raman spectroscopic studies." *J. Phys. Chem. B*, 101, pp. 9447–9457.
5. Hives I. and Thonstad J., 2004, "Electrical conductivity of low-melting electrolytes for aluminium smelting". *Electrochimica Acta*, 49, pp. 5111–5114.
6. Yang J., Hryn J., Davis B., Roy A., Krumdick G., and Pomukala J., 2004, "New opportunities for aluminum electrolysis with metal anodes in a low temperature electrolyte system." *Light Metals*, pp. 321–326.
7. Frazer E.J. and Thonstad J., 2010, "Alumina solubility and diffusion coefficient of the dissolved alumina species in the low-temperature fluoride electrolytes." *Metallurgical and Materials Transactions*, 41B, p. 543.
8. Apisarov A., Krukovsky V., Zaikov Y., Redkin A., Tkacheva O., and Khokhlov V., 2007, "Conductivity of low-temperature KF-AlF₃ electrolytes containing lithium fluoride and alumina." *Russian Journal of Electrochemistry* (English Translation), 43 (8), pp. 870–874.
9. Yang J., Graczyk D., Wunsch C., and Hryn J., 2007, "Alumina solubility in KF-AlF₃-based low temperature electrolyte system." *Light Metals*, pp. 537–541.
10. Yang J., Hryn J., and Krumdick G., 2006, "Aluminum electrolysis test with inert anodes in KF-AlF₃-based electrolyte." *Light Metals*, pp. 421–424.
11. Krukovsky V., Frolov A., Tkacheva O., Redkin A., Zaikov Y., Khokhlov V., and Apisarov A., 2006, "Electrical conductivity of the low melting cryolite melts." *Light Metals*, pp. 409–413.
12. Beck T., et al., 1991, U.S. Patent 5,006,209.
13. La Camera A., et al., 1995, U.S. Patent 5,415,742.
14. Beck T., et al., 2002, U.S. Patent 6,419,812 B1.
15. Wang J., Lai Y., Tian Z., and Liu Y., 2007, "Investigation of 5 Cu/(10 NiO-NiFe₂O₄) inert anode corrosion during low-temperature aluminum electrolysis." *Light Metals*, pp. 525–530.
16. Wang J., Lai Y., Tian Z., and Liu Y., 2007, "Effect of electrolysis superheat degree on anticorrosion performance of 5 Cu/(10 NiO-NiFe₂O₄) cermet inert anode." *J. Cent. South Univ. Technol.* pp. 768–772.

17. Lai Y., Huang L., Tian Z., Wang J., Zhang G., and Zhang Y., 2008, "Effect of CaO doping on corrosion resistance of Cu/(NiFe₂O₄-10 NiO) cermet inert anode for aluminum electrolysis." *J. Cent. South Univ. Technol.*, 15, pp. 743–747.
18. Li J., Fang Z., Lai Y., Lu X., and Tian Z., 2009, "Electrolysis expansion performance of semigraphitic cathode in [K₃AlF₆/Na₃AlF₆]-AlF₃-Al₂O₃ bath system." *J. Cent. South Univ. Technol.* 16, pp. 422–428.
19. Wang G., et al., 2011, "Corrosion behavior of cermet anodes in Na₃AlF₆-K₃AlF₆-based baths for low-temperature aluminum electrolysis cells," in *Supplemental Proceedings TMS*, 3, p. 175, San Diego, Calif.
20. Fang Z., Xu J., Hou J., Lo L., and Zhu J., 2012, "Electrolysis expansion performance of modified pitch based TiB₂-C composite cathode in [K₃AlF₆/Na₃AlF₆]-AlF₃-Al₂O₃ melts." *Light Metals*, pp. 1361–1365.
21. Zaikov Y., Chramov A., Kovrov V., Krukovsky V., Apisarov A., Tkacheva O., Chemezov O., and Shurov N., 2008, "Electrolysis of aluminum in the low melting electrolytes based on potassium cryolite." *Light Metals*, pp. 505–508.
22. Kovrov V., Chramov A., Redkin A., and Zaikov Y., 2009, "Oxygen evolving anodes for aluminum electrolysis." *ESC Transactions*, 16, pp. 7–17.
23. Chuikin A., and Zaikov Y., 2009, "Low-temperature electrolysis of aluminum in a bath made of corundum high-alumina concrete." *Metallurgy of Non-ferrous Metals*, 2, pp. 108–113.
24. Frolov A., Gusev A., Zaikov Y., Kataev A., Shurov N., Chuikin A., and Redkin A., 2009, "The effect of potassium cryolite on construction materials under electrolysis condition." *Light Metals*, pp. 1129–1133.
25. Khramov A.P., Kovrov V.A., Shurov N.I., and Zaikov Y.P., 2010, "Rate of metallic anode oxidation in the course of electrolysis of cryolite-alumina melts. Derivation of basic equations." *Russ. J. Electrochem.* (English Translation), 46 (6), pp. 659–664.
26. Kovrov V.A., Khramov A.P., Shurov N.I., and Zaikov Y.P., 2010 "Metal anodes oxidation rate forecasted by results of electrolysis." *Russ. J. Electrochem.* (English Translation), 46 (6), p. 665.
27. Kovrov V.A., Khramov A.P., Zaikov Y.P., Nekrasov V.N., and Ananyev M.V., 2011, "Studies on the oxidation rate of metallic inert anodes by measuring the oxygen evolved in low-temperature aluminium electrolysis." *J. Appl. Electrochem.*, 41 (11), pp. 1301–1309.
28. Apisarov A., Barreiro J., Dedyukhin A., Galan L., Redkin A., Tkacheva O., and Zaikov Y., 2012, "Reduction of the operating temperature of aluminum electrolysis: low temperature electrolyte." *Light Metals*, pp. 783–786.
29. Simakov D.A, Frolov A.V., and Gusev A.O., 2010, "Development of inert anodes for electrolysis." *Proceedings of the Second International Congress, "Non-Ferrous Metals – 2010,"* p. 354, Krasnoyarsk, Russia.
30. Beck T.R., MacRae C.M., and Wilson N.C., 2011, "Metal anode performance in low-temperature electrolytes for aluminum production." *Metallurgical and Materials Transaction B*, 42B, p. 807.

31. Brown C. W., 1998, "The wettability of TiB₂-based cathodes in low-temperature slurry-electrolyte reduction cells." *JOM*, p. 38.
32. Dedyukhin A., Apisarov A., Tkacheva O., Redkin A., and Zaikov Y., 2008, "Influence of CaF₂ on the properties of the low-temperature electrolyte based on the KF-AlF₃ (CR = 1,3) system." *Light Metals*, p. 505–508.
33. Dedyukhin A., Apisarov A., Redkin A., Tkacheva O., Zaikov Y., Nikolaeva E., and Tinghaev P., 2009, "Physical-chemical properties of the KF-NaF-AlF₃ molten system with low cryolite ratio." *Light Metals*, p. 401–403.
34. Dedyukhin A., Apisarov A., Redkin A., Tkacheva O., Zaikov Y., Frolov A., and Gusev A., 2009, "Electrical conductivity of the (KF-AlF₃)-NaF-LiF molten system with Al₂O₃ additions at low cryolite ratio." *ECS Transactions*, 16 (49), pp. 317–324.
35. Dedyukhin A., Apisarov A., Redkin A., Tkacheva O., and Zaikov Y., 2010, "Alumina solubility and electrical conductivity in potassium cryolites with low CR." *Molten Salts and Ionic Liquids: Never the Twain?* edited by M. Gaune-Escard and K. Seddon. John Wiley & Sons, Inc., pp. 75–84.
36. Apisarov A., Dedyukhin A., Nikolaeva E., Tin'ghaev P., Tkacheva O., Redkin A., and Zaikov Y., 2010, "Liquidus temperatures of cryolite melts with low cryolite ratio." *Light Metals*, pp. 395–398.
37. Apisarov A., Dedyukhin A., Nikolaeva E., Tin'ghaev P., Tkacheva O., Redkin A., and Zaikov Y., 2011, "Liquidus Temperatures of Cryolite Melts with Low Cryolite Ratio." *Metallurgical and Material Transaction B*, 42, pp. 236–242.
38. Wang J., Lai Y., Tian Z., Li J., and Liu Y., 2008, "Temperature of primary crystallization in party of system Na₃AlF₆-K₃AlF₆-AlF₃." *Light Metals*, pp. 513–518.
39. Huang Y., Lai Y., Tian Z., Li J., Liu Y., and Yi Q., 2008, "Electrical conductivity of (Na₃AlF₆-40 wt% K₃AlF₆)-AlF₃ melts." *Light Metals*, pp. 519–521.
40. Huang Y., Lai Y., Tian Z., Li J., Liu Y., and Yi Q., 2008, "Electrical conductivity of (Na₃AlF₆-40 wt% K₃AlF₆)-AlF₃ melts." *J. Cent. South Univ. Technol.*, 15, pp. 819–823.
41. Yan H., Yang J., and Li W., 2011, "Surface tension and density in the KF-NaF-AlF₃-based electrolyte." *J. Chem. Eng. Data*, 56, pp. 4147–4151.
42. Danielik V. and Gabcova J., 2004, "Phase diagram of the system KF-NaF-AlF₃." *J. Thermal Analysis and Calorimetry*, 76, p. 763.
43. Danielik V. and Hives J., 2004, "Low-melting electrolyte for aluminum smelting." *J. Chem. Eng. Data*, 49, pp. 1414–1417.
44. Silny A., Chrenkova M., Danek V., Vasiljev R., Nguyen D.K., and Thonstad J., 2004, "Density, viscosity, surface tension, and interfacial tension in the systems NaF(KF) + AlF₃." *J. Chem. Eng. Data*, 49, pp. 1542–1545.
45. Danielik V., 2005, "Phase equilibria in the system KF-AlF₃-Al₂O₃." *Chem. Pap.*, 59 (2), p. 81.
46. Chrenkova M., Silny A., Simko F., and Thonstad J., 2010, "Density of the NaAlF₄ + KAlF₄ electrolyte, saturated with alumina." *J. Chem. Eng. Data*, 55, pp. 3438–3440.

47. DOE-EERE ITP, 2007, U.S. Energy Requirements for Aluminum Production – Historical Perspectives, Theoretical Limits and Current Practices.
48. Burns, S., 2009, “Power costs in the production of primary aluminum,” *Metal Miner*.

APPENDIX A: OPERATING PARAMETERS

A-1 Operating parameters for the completed 20-A electrolysis tests

All experiments were performed in potassium-cryolite-based electrolytes with a cryolite ratio (CR) of 1.3 in a cell with one aluminum bronze anode and two wetted cathodes at an i_a (anode current density) of 0.45 A/cm^2 , i_c (cathode current density) of 0.52 A/cm^2 , and ACD (anode-to-cathode distance) of 2 cm or otherwise as specified. Table A-1 shows the operating parameters for the 20-A electrolysis tests.

Table A-1 Operating parameters for the completed 20-A electrolysis tests

Exp. No.	Electrolyte	Duration (h)	Temp. (°C)	Voltage (V, avg.)	Oxygen (% , avg.)	Current Efficiency (% , O/Al)	Cu in Produced Al (wt%)	Comments
E1	KF-AlF ₃ (CR = 1.37)	6	750	3.6	n.m.*	Low	n.m.	Electrolyte was overloaded with alumina, T _{Liq} = 623°C
E3	KF-AlF ₃ (CR = 1.37)	10	700	4.8	n.m.	n.m./30	n.m.	
E4	KF-AlF ₃ (CR = 1.37)	24	700	4.8	n.m.	n.m./40	1.5	T _{Liq} = 642°C
E5	KF-AlF ₃ + NaF (2 wt%, CR = 1.37)	24	730	4.6	n.m.	n.m./40	3.5	T _{Liq} = 705°C before electrolysis and 699°C after
E6	KF-AlF ₃ (CR = 1.37)	56	700	4.8	3.0	35/40	4.4	
E7	KF-AlF ₃ + NaF (4 wt%)	6	700	Reached 8.5 V		n.m.	n.m.	Voltage anomalies, T _{Liq} = 656°C
E8	KF-AlF ₃	24	700	3.5	5.0	65/75	0.7	T _{Liq} = 630°C
E9	KF-AlF ₃ + NaF (4 wt%)	26	750	3.5	5.0	65/80	0.8	Voltage oscillation, T _{Liq} = 662°C
EAL10	KF-AlF ₃	48	700	3.8	4.0	43/n.m.		Anode touched Al, voltage anomalies
EAL11	KF-AlF ₃	48	700	3.6	4.5	55/50	0.9	
EAL12	KF-AlF ₃	48	750	3.4	4.5	55/50	0.4	
EAL14	KF-AlF ₃ + NaF (2 wt%)	20	750	3.9	4.0	n.m.	0.8	Voltage anomalies, electrolyte was moisturized, O = 30%
EAL17	KF-AlF ₃ + NaF (2 wt%)	11	750	3.4	4.3	50/50	0.4	
EAL18	KF-AlF ₃ + NaF (4 wt%)	18	770	3.75	4.0	50/50	3.4	Substantial voltage oscillation

Table A-1 (Cont.)

Exp. No.	Electrolyte	Duration (h)	Temp. (°C)	Voltage (V, avg.)	Oxygen (% , avg.)	Current Efficiency (% , O/Al)	Cu in Produced Al (wt%)	Comments
EAL19	KF-AlF ₃ + NaF (2 wt%)	56	750	3.4	5.0	62/67	0.9	
EAL21	KF-AlF ₃ + NaF (4 wt%)	34	770	3.5	3.5	44/47	2.4	Voltage anomalies
EAL22	KF-AlF ₃	74	730	3.8	5.3	70/80	6-8	Currents of 10, 15, and 20 A, anode corrosion
EAL23	KF-AlF ₃	52	715	3.75	4.0	50/n.m.	0.4	Stainless steel leads to anode were destroyed
EAL24	KF-AlF ₃	32	700	3.3	5.0	62/66	0.3	
E25	KF-AlF ₃	70	715	3.6	4.2	51/57	0.5	
E26	KF-AlF ₃	96	700	3.55	5.0	55/54	0.7	
E29	KF-AlF ₃	30	700	3.6	6-3.5	60/64	0.8	One cathode and two anodes, T _{liq} = 633°C, i _c = 0.67 A/cm ² , i _a = 0.45 A/cm ²
E30	KF-AlF ₃	62	700	3.6	6.3-4	62/n.m.	1.8	One cathode and two anodes, both anodes fell in melt, i _c = 0.67 A/cm ² , i _a = 0.45 A/cm ²
EAL31	KF-AlF ₃	30	750	3.4-4.0	4.0-8.0	50/60	0.4	Currents of 15, 20, and 25 A
EAL33	KF-AlF ₃	83	715	3.8	5-2	38/60	n.m.	Cathodes – four rods, one anode, “semi-immersed” anode, i _c = 0.6 A/cm ² , i _a = 0.45 A/cm ²
E36	KF-AlF ₃	56	750	3.5	6.0	50/60	0.7	Semi-immersed anode, voltage anomalies
EAL38	KF-AlF ₃	46	750	3.4	Ar or N ₂ rate changed	62/60	0.15	
30E39	KF-AlF ₃	51	750	3.6	n.m.	n.m./75	0.7	Current of 30 A, i _a = 0.5 A/cm ² , i _c = 0.74 A/cm ²

Table A-1 (Cont.)

Exp. No.	Electrolyte	Duration (h)	Temp. (°C)	Voltage (V, avg.)	Oxygen (% , avg.)	Current Efficiency (% , O/Al)	Cu in Produced Al (wt%)	Comments
EAL40	KF-AlF ₃	44	750	4–6	2.5	n.m./66	0.5	One anode and four rods immersed in Al pool, $i_a = 0.45 \text{ A/cm}^2$, $i_c = 0.25 \text{ A/cm}^2$, voltage anomalies
EAL43	KF-AlF ₃	76	750	3.4–5.0	4.0–8.0 (N ₂ = 0.5 L/min)	50/60	0.65	Currents of 15, 20, and 25 A; anode was protected from contact with vapors before test
EAL44	KF-AlF ₃	51	750	3.3	6.0 (N ₂ = 0.5 L/min)	72/80	0.4	$i_a = 0.4 \text{ A/cm}^2$, anode was protected from contact with vapors before test
EAL45	KF-AlF ₃	56	750	3.6	10.0 (N ₂ = 0.5 L/min)	78/78	0.4	$i_a = 0.6 \text{ A/cm}^2$, anode was protected from contact with vapors before test
* n.m. = not measured.								

A-2 Operating parameters for the completed 100-A electrolysis tests

All experiments were performed in the KF-AlF₃ electrolyte with a CR of 1.3 in a cell with one aluminum bronze anode and two wetted cathodes at an i_a of 0.45 A/cm², i_c of 0.52 A/cm², and ACD of 2 cm or otherwise as specified. Table A-2 shows the operating parameters for the 100-A electrolysis tests.

Table A-2 Operating parameters for the completed 100-A electrolysis tests

Exp. No.	Electrolyte	Duration (h)	Temp. (°C)	Voltage (V, avg.)	Oxygen (% avg.)	Current Efficiency (% O/Al)	Cu in Produced Al (wt%)	Comments
100E27	KF-AlF ₃	25	750	3.8	n.m.*	n.m./70	0.5	T _{liq} = 632°C
100E28	KF-AlF ₃	57	730	3.9	n.m.	n.m./46	3.0	Voltage anomalies
100E34	KF-AlF ₃	100	750	3.8	n.m.	n.m./50	3.0	Voltage anomalies
100E35	KF-AlF ₃	28	750	7.8	n.m.	n.m./25	10	One cathode and one anode, ACD = 7 cm
100E37	KF-AlF ₃	82	750	4	n.m.	n.m./70	0.15	I _a = 0.45 A/cm ² , I _c = 0.7 A/cm ²
100E41	KF-AlF ₃	106	750	4	20	46/50	1.6	Anode was protected from contact with vapors before test
* n.m. = not measured.								



Argonne National Laboratory

9700 South Cass Avenue

Argonne, IL 60439

www.anl.gov



Argonne National Laboratory is a U.S. Department of Energy
laboratory managed by UChicago Argonne, LLC